THE JOURNAL OF BIOLOGICAL CHEMISTRY VOL. 290, NO. 5, pp. 2919–2937, January 30, 2015

A Novel Phosphatidylinositol 4,5-Bisphosphate Binding Domain Mediates Plasma Membrane Localization of ExoU and Other Patatin-like Phospholipases*

Received for publication, September 13, 2014, and in revised form, November 26, 2014 Published, JBC Papers in Press, December 10, 2014, DOI 10.1074/jbc.M114.611251

Gregory H. Tyson[‡1], Andrei S. Halavaty[§¶], Hyunjin Kim[‖], Brett Geissler[‡2], Mallory Agard[‡], Karla J. Satchell[‡], Wonhwa Cho[‖], Wayne F. Anderson[§¶], and Alan R. Hauser[‡3]**

*From the Departments of [‡]Microbiology-Immunology, **Medicine, and [§]Biochemistry and [¶]Center for Structural Genomics of Infectious Diseases, Northwestern University, Chicago, Illinois 60611 and the [‖]Department of Chemistry, University of Illinois at Chicago, Chicago, Illinois 60607*

Background: The *Pseudomonas aeruginosa* cytotoxin ExoU localizes to the plasma membrane in eukaryotic cells.
Results: ExoU and related proteins utilize a conserved four-helical bundle to bind the lipid phosphatidylinositol 4,5-bisphosphate for localization.
Conclusion: The membrane localization domain of ExoU represents a novel phosphoinositide binding domain.
Significance: This is the first report of a four-helical bundle with specificity for phosphatidylinositol 4,5-bisphosphate.

Bacterial toxins require localization to specific intracellular compartments following injection into host cells. In this study, we examined the membrane targeting of a broad family of bacterial proteins, the patatin-like phospholipases. The best characterized member of this family is ExoU, an effector of the *Pseudomonas aeruginosa* type III secretion system. Upon injection into host cells, ExoU localizes to the plasma membrane, where it uses its phospholipase A_2 activity to lyse infected cells. The targeting mechanism of ExoU is poorly characterized, but it was recently found to bind to the phospholipid phosphatidylinositol 4,5-bisphosphate ($PI(4,5)P_2$), a marker for the plasma membrane of eukaryotic cells. We confirmed that the membrane localization domain (MLD) of ExoU had a direct affinity for $PI(4,5)P_2$, and we determined that this binding was required for ExoU localization. Previously uncharacterized ExoU homologs from *Pseudomonas fluorescens* and *Photorhabdus asymbiotica* also localized to the plasma membrane and required $PI(4,5)P_2$ for this localization. A conserved arginine within the MLD was critical for interaction of each protein with $PI(4,5)P_2$ and for localization. Furthermore, we determined the crystal structure of the full-length *P. fluorescens* ExoU and found that it was similar to that of *P. aeruginosa* ExoU. Each MLD contains a four-helical bundle, with the conserved arginine exposed at its cap to allow for interaction with the negatively charged $PI(4,5)P_2$. Overall, these findings provide a structural explanation for the targeting of patatin-like phospholipases to the plasma membrane and define the MLD of ExoU as a member of a new class of $PI(4,5)P_2$ binding domains.

Bacteria use a number of mechanisms to inject toxins into eukaryotic cells (1). Once inside these cells, the toxins perform a variety of functions to disrupt host cell physiology (2–4). To adequately perform these functions, it is critical that toxins are localized to the appropriate intracellular compartment. A number of bacterial toxins have dedicated membrane localization domains (MLDs)[4] that vary considerably in their targeting specificities and mechanisms (5). For instance, the botulinum neurotoxin A concentrates at the plasma membrane of neurons by direct affinity to the protein SNAP-25 (6). Other proteins localize to different membrane compartments by undergoing covalent lipid modification, such as the *Salmonella* effector SifA, which targets the plasma membrane following farnesylation (7). Still other proteins, such as the *Pasteurella multocida* toxin, have direct affinity for lipids (8). The many sophisticated and resourceful mechanisms by which bacterial toxins undergo intracellular targeting underscore the importance of proper localization to toxin function (7, 9). Although the examples listed above illustrate several well characterized mechanisms of toxin localization, it remains unclear how the majority of bacterial toxins are targeted to the appropriate intracellular compartment.

Patatin-like phospholipases are an important and intriguing family of microbial proteins. They are defined by the presence

* This work was supported, in whole or in part, by National Institutes of Health Grants AI053674, AI075191, AI099269, AI04831, and AI088286 (to A. R. H.) and AI092825 and AI051490 (to K. J. S.). This work was also supported by American Heart Association Grant 12PRE8660003 (to G. H. T.).
The atomic coordinates and structure factors (code 4QMK) have been deposited in the Protein Data Bank (http://wwpdb.org/).
[1] Present address: Food and Drug Administration, Laurel, MD 20708.
[2] Present address: Nalco Champion, Sugar Land, TX 77478.
[3] To whom correspondence should be addressed: Depts. of Microbiology-Immunology and of Medicine, Northwestern University, 303 E. Chicago Ave., Chicago, IL 60611. Tel.: 312-503-1044; Fax: 312-503-1339; E-mail: ahauser@northwestern.edu.

[4] The abbreviations used are: MLD, membrane localization domain; PC, phosphatidylcholine; PE, phosphatidylethanolamine; PS, phosphatidylserine; PI, phosphatidylinositol; PI(4)P, phosphatidylinositol 4-phosphate; PI(5)P, phosphatidylinositol 5-phosphate; $PI(4,5)P_2$, phosphatidylinositol 4,5-bisphosphate; $PI(3,4,5)P_3$, phosphatidylinositol 3,4,5-triphosphate; PLA_2, phospholipase A_2; SPR, surface plasmon resonance; PMT, *P. multocida* toxin; FERM, 4.1/ezrin/radixin/moesin; BPD, bacterial phosphoinositide binding domain; PH, pleckstrin homology; $cPLA_2$, cytosolic PLA_2; $ExoU_{P.\ aer}$, ExoU from *P. aeruginosa*; $ExoU_{P.\ flu}$, ExoU from *P. fluorescens*; $ExoU_{P.\ asy}$, ExoU from *P. asymbiotica*; BisTris, 2-[bis(2-hydroxyethyl)amino]-2-(hydroxymethyl)propane-1,3-diol.

of a patatin domain, which encodes for phospholipase A_2 (PLA_2) activity that cleaves phospholipids at the *sn*-2 position (4). Patatin-like phospholipases are closely related to eukaryotic group IV cytosolic PLA_2 ($cPLA_2$) and group VI calcium-independent PLA_2 enzymes, which share a defined serine-aspartate catalytic dyad (10, 11). While only recently identified, this family of proteins is quite large; ~4400 potential proteins containing typical patatin domains are encoded in sequenced bacterial genomes (12, 13). Only a few of these proteins have been characterized, but these limited studies have found that patatin-like phospholipases can be delivered by type III, type IV, or type V secretion systems into host cells (11, 14, 15). Once in the eukaryotic intracellular environment, the PLA_2 activities are associated with host cell death, disruption of signaling pathways, and bacterial internalization (15, 16, 18).

Arguably, the best characterized member of the family of patatin-like phospholipases is ExoU of *Pseudomonas aeruginosa*. This protein was initially discovered based upon its ability to confer cytotoxicity to *P. aeruginosa* strains and its secretion by the type III secretion system (19–21). Subsequent studies have defined it as one of the predominant virulence determinants of *P. aeruginosa*, as the secretion of ExoU is associated with poor clinical outcomes in human patients and with more severe infection in animal models (22, 23). ExoU does not act as a PLA_2 enzyme on its own but instead requires eukaryotic host cofactors to be activated (24). Ubiquitin and ubiquitinated proteins have been identified as important for the activation of ExoU (25), as has the lipid phosphatidylinositol 4,5-bisphosphate ($PI(4,5)P_2$) (26). Together, ubiquitin and $PI(4,5)P_2$ activate ExoU synergistically, with each being important to the cytotoxic action of ExoU (26).

The C-terminal MLD of ExoU is necessary and sufficient for targeting of this effector protein to the plasma membrane (27). The crystal structure of ExoU in complex with its bacterial chaperone SpcU revealed that the MLD region encompasses residues 503–687 (28, 31). Furthermore, the C-terminal half (residues 604–687) of the MLD forms a four-helical bundle, a structural motif used by other toxins to target the plasma membrane (8, 29). Several key residues within the four-helical bundle have been identified as being critical to ExoU localization (27, 30), but the mechanism by which the MLD specifically recognizes the plasma membrane is unclear. Interestingly, it was recently shown that purified recombinant ExoU bound to $PI(4,5)P_2$ immobilized on a solid support and that this binding required the MLD (31). Subsequent work has established that ExoU has a high affinity for $PI(4,5)P_2$ and can use $PI(4,5)P_2$ as a substrate (32). $PI(4,5)P_2$ is a phospholipid found in the inner leaflet of the plasma membrane of eukaryotic cells (but not bacteria) (33), where it is recognized as a "signpost" to appropriately direct a number of endogenous proteins to this intracellular compartment (34). To dock at the plasma membrane, these proteins use a number of well characterized $PI(4,5)P_2$ binding domains (*e.g.* pleckstrin homology, PSD-95/Dlg/ZO-1, and FERM domains), which play important roles in numerous cellular processes (35, 36). Although ExoU does not contain a known $PI(4,5)P_2$ binding domain, its high affinity for $PI(4,5)P_2$ has led others to hypothesize that it may localize to the plasma membrane by binding $PI(4,5)P_2$ (31, 32). Thus, it is conceivable that the MLD of ExoU contains a novel $PI(4,5)P_2$ binding domain.

In this study, we demonstrate that ExoU localizes to the plasma membrane through direct binding of the MLD to $PI(4,5)P_2$. We extended these findings to patatin-like phospholipases of *Pseudomonas fluorescens* and *Photorhabdus asymbiotica,* demonstrating that the MLD of ExoU is a domain used by proteins of other bacterial genera and species to target the plasma membrane. To gain more information about this family of MLDs, we determined the crystal structure of the ExoU homolog of *P. fluorescens.* This structure was used along with the previously determined structure of *P. aeruginosa* ExoU to show that the four-helical bundle is conserved within the MLD and is positioned to expose a conserved positively charged arginine residue to interact with the negatively charged phosphate groups of $PI(4,5)P_2$ in the plasma membrane. These results define a novel $PI(4,5)P_2$ binding domain used by bacterial proteins to target the plasma membrane of host cells.

EXPERIMENTAL PROCEDURES

Cell Lines, Bacterial and Yeast Strains, and Media—Bacterial and yeast strains are listed in Tables 1 and 2, respectively. *Escherichia coli* strains were grown in Luria-Bertani (LB) broth, and when appropriate, media were supplemented with 100 μg/ml ampicillin. *P. fluorescens* strain A506 was a generous gift from Joyce Loper. *P. asymbiotica* strain ATCC 43949 was acquired from the ATCC. *Saccharomyces cerevisiae* strains SEY6210 (wild-type) and Δ*inp54*/Δ*sac1,* which were generous gifts from Peter Mayinger, were grown in yeast extract peptone dextrose (YPD) medium. Yeast strains expressing glucose-repressible, galactose-inducible pYC vectors were grown in synthetic complete medium lacking uracil and supplemented with 2% glucose (SC-ura + Glu) or 2% galactose, 1% raffinose (SC-ura + Gal) for varied expression of proteins (26). HeLa cells were cultured in modified Eagle's medium supplemented with 10% fetal bovine serum (Invitrogen).

Purification of ExoU and Its Homologs—*P. fluorescens* and *P. asymbiotica* were grown overnight in LB broth, and genomic DNA was isolated with the DNeasy blood and tissue kit (Qiagen). Primers containing HindIII and NotI sites were used to amplify the *exoU* gene homolog from each species. (All primers used in this study are listed in Table 3.) PCR amplification products and the HN-C expression vector (Clontech) were digested with HindIII and NotI restriction enzymes, and the products were ligated and transformed into BL21 (DE3) Star competent cells. (All plasmids used in this study are listed in Tables 1 and 2.) ExoU proteins were purified as described previously using a HisTrap FF nickel column and a HiPrep 26/10 desalting column (GE Healthcare) (26). For purification of MLD proteins, corresponding primers were used to amplify the portion of the gene encoding the MLD, and amplification products were digested with HindIII and NotI. The digested products were ligated into a similarly digested HN-N vector (Clontech), and the ligated construct was transformed into BL21 (DE3) Star competent cells. Purification of these proteins was performed as described above.

HeLa Cell Cytotoxicity Assays—ExoU proteins were expressed in HeLa cells by transfection of expression vectors. Constructs

TABLE 1
Bacterial strains and plasmids

Name	Relevant characteristics	Ref./Source
P. fluorescens A506	Contains *exoU* homolog	Loper *et al.* (60)
P. asymbiotica ATCC 43949	Contains *exoU* homolog	ATCC
***E. coli* strains**		
Top10	F− *mcr*A Δ(*mrr-hsd*RMS-*mcr*BC) φ80*lac*ZΔM15 Δ*lac*X74 *rec*A1 *ara*D139 Δ(*ara-leu*)7697 *gal*U *gal*K *rps*L (StrR) *end*A1 *nup*G	Invitrogen
BL21	F-*ompT hsdS*$_B$ (r_B-m_B-) *gal dcm* (DE3)	Invitrogen
***E. coli* Purification Plasmids**		
pEcoli-Cterm 6×HN	*E. coli* purification vector with C-terminal HN tag; Amp^r	Clontech
pEcoli-Nterm 6×HN	*E. coli* purification vector with N-terminal HN tag; Amp^r	Clontech
pEcoli-Cterm 6×HN-ExoU$_{P.aer}$	For purification of full-length ExoU$_{P.aer}$	30
pEcoli-Cterm 6×HN-ExoU$_{P.flu}$	For purification of full-length ExoU$_{P.flu}$	This study
pEcoli-Cterm 6×HN-ExoU$_{P.asy}$	For purification of full-length ExoU$_{P.asy}$	This study
pEcoli-Nterm 6×HN-ExoU$_{P.aer}$ MLD	For purification of ExoU$_{P.aer}$ MLD (503–687)	This study
pEcoli-Nterm 6×HN-ExoU$_{P.aer}$ MLD (LS608)	ExoU$_{P.aer}$ MLD construct with LS608 linker insertion	This study
pEcoli-Nterm 6×HN-ExoU$_{P.aer}$ MLD (I609N)	ExoU$_{P.aer}$ MLD construct with I609N substitution	This study
pEcoli-Nterm 6×HN-ExoU$_{P.aer}$ MLD (Q623R)	ExoU$_{P.aer}$ MLD construct with Q623R substitution	This study
pEcoli-Nterm 6×HN-ExoU$_{P.aer}$ MLD (N627I)	ExoU$_{P.aer}$ MLD construct with N627I substitution	This study
pEcoli-Nterm 6×HN-ExoU$_{P.aer}$ MLD (I654N)	ExoU$_{P.aer}$ MLD construct with I654N substitution	This study
pEcoli-Nterm 6×HN-ExoU$_{P.aer}$ MLD (R661L)	ExoU$_{P.aer}$ MLD construct with R661L substitution	This study
pEcoli-Nterm 6×HN-ExoU$_{P.aer}$ MLD (A678D)	ExoU$_{P.aer}$ MLD construct with A678D substitution	This study
pEcoli-Nterm 6×HN-ExoU$_{P.flu}$ MLD	For purification of ExoU$_{P.flu}$ MLD (453–639)	This study
pEcoli-Nterm 6×HN-ExoU$_{P.flu}$ MLD (R616L)	ExoU$_{P.flu}$ MLD construct with R616L substitution	This study
pEcoli-Nterm 6×HN-ExoU$_{P.asy}$ MLD	For purification of ExoU$_{P.asy}$ MLD (495–676)	This study
pEcoli-Nterm 6×HN-ExoU$_{P.asy}$ MLD (R652L)	ExoU$_{P.asy}$ MLD construct with R652L substitution	This study
***E. coli* transfection plasmids**		
pcDNA3.1 NT-GFP	Mammalian expression plasmid with N-terminal GFP tag; Amp^r	Invitrogen
pcDNA3.1 ExoU$_{P.aer}$ MLD-GFP	Plasmid for expression of ExoU$_{P.aer}$ MLD-GFP	This study
pcDNA3.1 ExoU$_{P.aer}$ MLD (R661L)-GFP	ExoU$_{P.aer}$ MLD construct with R661L substitution	This study
pcDNA3.1 ExoU$_{P.flu}$ MLD-GFP	Plasmid for expression of ExoU$_{P.flu}$ MLD-GFP	This study
pcDNA3.1 ExoU$_{P.flu}$ MLD (R616L)-GFP	ExoU$_{P.flu}$ MLD construct with R616L substitution	This study
pcDNA3.1 ExoU$_{P.asy}$ MLD-GFP	Plasmid for expression of ExoU$_{P.asy}$ MLD-GFP	This study
pcDNA3.1 ExoU$_{P.asy}$ MLD (R652L)-GFP	ExoU$_{P.asy}$ MLD construct with R652L substitution	This study
pcDNA3.1 ExoU$_{P.aer}$-GFP	Plasmid for expression of ExoU$_{P.aer}$ in mammalian cells	65
pcDNA3.1 ExoU$_{P.aer}$-S142A-GFP	pcDNA3.1 ExoU$_{P.aer}$-GFP with S142A substitution	65
pcDNA3.1 ExoU$_{P.flu}$-GFP	For expression of ExoU$_{P.flu}$-GFP in mammalian cells	This study
pcDNA3.1 ExoU$_{P.flu}$-S92A-GFP	pcDNA3.1 ExoU$_{P.flu}$-GFP with S92A substitution	This study
pcDNA3.1 ExoU$_{P.asy}$-GFP	For expression of ExoU$_{P.asy}$-GFP in mammalian cells	This study
pcDNA3.1 ExoU$_{P.asy}$-S137A-GFP	pcDNA3.1 ExoU$_{P.asy}$-GFP with S137A substitution	This study

TABLE 2
***S. cerevisiae* strains and plasmids**

Name	Relevant characteristics	Ref./Source
***S. cerevisiae* strains**		
Wild-type (SEY6210)	*MATα trp-Δ901 leu2-3, 112 his3-Δ200 ura3-52 lys2-801 suc2-Δ9 can1::hisG*	Mayinger and co-workers (81)
Δ*inp54*/Δ*sac1*	*MATα trp-Δ901 leu2–3, 112 his3- Δ200 ura3–52 lys2–801 suc2-Δ9 can1::hisG sac1::TRP1, inp54::LEU2*	Mayinger and co-workers (61)
***S. cerevisiae* plasmids**		
pYC2/NT A	Glu-repressible, Gal-inducible yeast expression vector	Invitrogen
pYC-ExoU$_{P.aer}$-S142A-GFP	For expression of ExoU$_{P.aer}$-S142A-GFP	This study
pYC-ExoU$_{P.flu}$-S92A-GFP	For expression of ExoU$_{P.flu}$-S92A-GFP	This study
pYC-ExoU$_{P.asy}$-S137A-GFP	For expression of ExoU$_{P.asy}$-S137A-GFP	This study
pYC-ExoU$_{P.asy}$ MLD-GFP	For expression of ExoU$_{P.asy}$ MLD-GFP	This study
pYC-2x(GFP-PH)	For expression of GFP-tagged pleckstrin homology domain from PLCδ	Orth and co-workers (72)

expressing wild-type ExoU from *P. aeruginosa* (hereafter referred to as ExoU$_{P. aer}$) and variants containing amino acid substitutions had previously been generated using plasmid pcDNA3.1 NT-GFP (30). To generate similar constructs expressing ExoU homologs from *P. fluorescens* and *P. asymbiotica* (ExoU$_{P. flu}$ and ExoU$_{P. asy}$, respectively) primers containing flanking AgeI and NotI sites were used to amplify the ExoU-encoding genes from the respective purification vectors. Then the pcDNA3.1 NT-GFP vector (Invitrogen) and the PCR products were digested with AgeI and NotI. The digested products were purified, ligated, and transformed into *E. coli* Top10 cells. The catalytic site substitutions were engineered by site-directed mutagenesis of *exoU*$_{P. flu}$ and *exoU*$_{P. asy}$ using the QuikChange site-directed mutagenesis kit (Agilent) (30) and the primers listed in Table 3. The constructs encoding the R661L substitution in ExoU$_{P. aer}$ and the corresponding substitutions in ExoU$_{P. flu}$ and ExoU$_{P. asy}$ were similarly engineered in the pcDNA plasmids by site-directed mutagenesis using primers listed in Table 3. Plasmids were purified using the QIAprep spin miniprep kit (Qiagen). X-treme gene transfection reagent (Roche Applied Science) was coupled with the DNA transfection constructs in serum-free medium to perform transfections with HeLa cells as described previously (30). Medium was collected after 24 h and measured for lactate dehydrogenase activity using the Cytotox 96 nonradioactive cytotoxicity assay (Promega).

Immunoblot Analysis for Detection of GFP-tagged Proteins—The same constructs used in the HeLa cell cytotoxicity assays were used for expression of GFP-tagged ExoU proteins from the pcDNA3.1 NT-GFP vector. Lipofectamine 2000 (Invitrogen) was coupled with DNA in serum-free medium and trans-

TABLE 3
Primers used in this study

Name	Sequence (5′ → 3′)[a]
For purification	
5′ ExoU$_{P.aer}$ MLD HindIII	AAA**AAGCTT**ATCACAGACGGGGCGGTG
3′ ExoU$_{P.aer}$ MLD NotI	AAA**GCGGCCGC**CTGTGAACTCCTTATTCCG
5′ ExoU$_{P.flu}$ HindIII	AAA**AAGCTT**ATGAAAGTCTCCAGTTCT
3′ ExoU$_{P.flu}$ NotI	AAA**GCGGCCGC**CAACCGGAATACGCCAGGC
5′ ExoU$_{P.flu}$ MLD HindIII	AAA**AAGCTT**GCCGGCGCCGAGGCGTTG
5′ ExoU$_{P.asy}$ HindIII	AAA**AAGCTT**ATGCAAATTCACATTAAT
3′ ExoU$_{P.asy}$ NotI	AAA**GCGGCCGC**CTGCTGTTTTGATCATCCA
5′ ExoU$_{P.asy}$ MLD HindIII	AAA**AAGCTT**TCAACCTCAAACATTGCT
For transfection	
5′ ExoU$_{P.flu}$ AgeI	AAA**ACCGGT**GATGAAAGTCTCCAGTTCT
3′ ExoU$_{P.flu}$ NotI	AAA**GCGGCCGC**CCTAAACCGGAATACGCCA
5′ ExoU$_{P.asy}$ AgeI	AAA**ACCGGT**GATGCAAATTCACATTAAT
3′ ExoU$_{P.asy}$ NotI	AAA**GCGGCCGC**CCTATGCTGTTTTGATCAT
5′ ExoU$_{P.aer}$ MLD AgeI	AAA**ACCGGT**GATCACAGACGGGGCGGTG
3′ ExoU$_{P.aer}$ NotI	AAA**GCGGCCGC**CTCATGTGAACTCCTTATT
5′ ExoU$_{P.flu}$ MLD AgeI	AAAACCGGTGGCCGGCGCCGAGGCGTTG
5′ ExoU$_{P.asy}$ MLD AgeI	AAAACCGGTGTCAACCTCAAACATTGCT
For site-directed mutagenesis	
5′ ExoU$_{P.flu}$ S92A	GTGGTTTCCGGCTCAGCGGCCGGTGCGATTTG
3′ ExoU$_{P.flu}$ S92A	CAAATCGCACCGGCCGCTGAGCCGGAAACCAC
5′ ExoU$_{P.flu}$ R616L	GTCAAACATTACCGAGCGCTCAATAAACCCTGGAGTAAAC
3′ ExoU$_{P.flu}$ R616L	GTTTACTCCAGGGTTTATTGAGCGCTCGGTAATGTTTGAC
5′ ExoU$_{P.asy}$ S137A	CACCATGTCAGGTTCTGCTGCGGGCGGGATCAC
3′ ExoU$_{P.asy}$ S137A	GTGATCCCGCCCGCAGCAGAACCTGACATGGTG
5′ ExoU$_{P.asy}$ R652L	GGCGGACAATTATGGCGCACTAATGAAACCTTGGAAAAAAC
3′ ExoU$_{P.asy}$ R652L	GTTTTTTCCAAGGTTTCATTAGTGCGCCATAATTGTCCGCC
For yeast cloning	
5′ GFP yeast	GACTCACTATAGGGAATATTAAGCTTACCATGGCCAGCAAAGGAGAAGAA
3′ ExoU$_{P.aer}$	GATAGGCTTACCTTCGAAGGGCCCTCTAGATCATGTGAACTCCTTATTCC
3′ ExoU$_{P.flu}$	GATAGGCTTACCTTCGAAGGGCCCTCTAGACTAAACCGGAATACGCCAGG
3′ ExoU$_{P.asy}$	GATAGGCTTACCTTCGAAGGGCCCTCTAGACTATGCTGTTTTGATCATCC

[a] Restriction sites are in bold.

fected onto 10-cm dishes of HeLa cells. After 24 h, cells were washed, collected, and lysed as described previously (26). Samples were run on a 10% SDS-polyacrylamide gel, transferred to a nitrocellulose membrane, and incubated in blocking buffer for 2 h at room temperature, as described previously (26). The membrane was incubated overnight at 4 °C with gentle shaking in the presence of Living Colors A.v. monoclonal antibody (Clontech) diluted 1:3000 in blocking buffer with 0.1% Tween 20. The membrane was washed and incubated with goat anti-mouse secondary antibody IR dye 800 (Li-Cor Biosciences) diluted 1:10,000 in blocking buffer supplemented with 0.1% Tween 20, for 1 h at room temperature with gentle shaking. The membrane was washed again, and blots were imaged using the Li-Cor Odyssey system.

HeLa Cell Fluorescence Microscopy—As described for the cytotoxicity assays, the MLD-encoding portions of *exoU* genes (both wild-type alleles and those encoding arginine-to-leucine substitutions) were amplified by PCR from the pcDNA3.1 NT-GFP ExoU constructs. The PCR product and the pcDNA3.1 NT-GFP vector were digested with AgeI and NotI, ligated, and transformed into Top10 cells. Expression constructs were purified using QIAprep spin miniprep kit. One day prior to transfection, HeLa cells were seeded into 24-well dishes containing coverslips. Cells were transfected as described for cytotoxicity assays and incubated for 20 h. Coverslips were washed and fixed in 3.7% formaldehyde and transferred to slides containing Prolong Gold anti-fade reagent (Molecular Probes). Coverslips were sealed with nail polish and visualized using a Nikon C2+ multispectral laser scanning confocal microscope at the Northwestern University Cell Imaging Facility. HeLa cell images were analyzed for fluorescence intensity distribution across individual cells using ImageJ version 1.43 software (National Institutes of Health).

Construction of Yeast Plasmids—Alleles encoding the catalytic variants of each of the ExoU homologs were PCR-amplified from the pcDNA3.1 NT-GFP vectors. The *exoU*$_{P.\ asy}$ MLD was similarly amplified. A pYC2/NT A vector (Invitrogen), which contains a glucose-repressible, galactose-inducible promoter (37), was digested with HindIII and XbaI. Using the LiAc heat shock method (37), 15 μl of PCR product and 1 μl of digested plasmid DNA were ligated within *S. cerevisiae* wild-type and Δ*inp54*/Δ*sac1* strains, and appropriate colonies were selected on synthetic complete medium lacking uracil.

Visualization of Yeast Strains—Yeast strains were grown in SC-ura + Gal medium to induce expression of the GFP-tagged constructs. Yeast were immobilized in 1% agarose solution on coverslips and visualized using a Nikon C2+ multispectral laser scanning confocal microscope.

Liposome Binding Assays—Liposome binding assays were performed as described previously (38). Briefly, a neutral lipid backbone was prepared with 30% phosphatidylcholine (PC), 20% phosphatidylethanolamine (PE), and 20% cholesterol (Avanti Polar Lipids). The remaining lipids were 30% PC, 30% PE, 30% phosphatidylserine (PS), 30% phosphatidylinositol, or a combination of 25% PC with 5% phosphatidylinositol, PI(4)P, PI(5)P, PI(4,5)P_2, or PI(3,4,5)P_3. These lipids were mixed as chloroform stocks that were dried under nitrogen gas and then by vacuum. Lipids were resuspended in liposome buffer (100 mM KCl, 1 mM $MgCl_2$, and 1 mM $CaCl_2$ in 20 mM HEPES (pH 7.5)) to a final concentration of 3 mM and sonicated. ExoU pro-

tein was added to a final concentration of 3 μM (38). Protein and liposomes were coincubated at 37 °C for 5 min. Ultracentrifugation was then performed at 200,000 × *g* for 2 h at 25 °C. The supernatants were removed, and the pellets were resuspended in an equal volume of liposome buffer. Samples were run on 4–15% gradient SDS-polyacrylamide gels, and proteins were visualized by Coomassie staining. Band intensity was analyzed using ImageJ version 1.43 software.

PLA_2 Assays—PLA_2 assays were performed using the Cayman Chemical $cPLA_2$ kit as described previously (26). Briefly, a total of 65 pmol of ExoU was added to 200 μl of 1.5 mM arachidonoyl thiophosphatidylcholine substrate for each assay condition. When indicated, 65 pmol of $PI(4,5)P_2$ (Avanti Polar Lipids) or 1.3 nmol of 55% PC, 20% PE, 20% cholesterol, and 5% $PI(4,5)P_2$-containing liposomes were added. In addition, 65 pmol or 65 fmol of ubiquitin (Sigma) were added when indicated. Absorbance was measured at 405 nm at the times indicated after the addition of 10 μl of 25 mM 5,5′-dithiobis(2-dinitrobenzoic acid). The PLA_2 activity of ExoU was calculated using the following formula: $A_{405}/10.00 \times 1/(\text{nmol of ExoU})$, where 10.00 is the extinction coefficient for 5,5′-dithiobis(2-dinitrobenzoic acid).

Protein BLAST Analysis—Nonredundant protein sequences were analyzed for similarity to $ExoU_{P.\ aer}$ (UniProtKB accession number O34208) by performing protein-protein BLAST searches (39). MLD similarity was based upon $ExoU_{P.\ aer}$ residues 503–687, and homologs from different bacterial species were analyzed for alignment of key residues.

Surface Plasmon Resonance (SPR) Analysis—SPR analysis was performed on a BIAcore X instrument with a lipid-coated L1 chip as described previously (40). Lipids were prepared by mixing chloroform stocks and then drying them under nitrogen gas. Lipids were resuspended in 160 mM NaCl in 20 mM Tris (pH 7.4) to a final concentration of 400 μg/ml, sonicated, and extruded for uniform 100 nm liposome size. Kinetic and equilibrium SPR measurements were performed with the flow rate set at 30 and 10 μl/ml, respectively. Experiments determining K_d values were performed in triplicate. PC vesicles, to which ExoU has no detectable affinity, were used for the control surface. The active surface was coated with liposomes containing 77% PC, 20% PS, and 3% phosphoinositides or with 97% PC and 3% phosphoinositides. Assuming a Langmuir-type binding between the protein and protein-binding sites on vesicles, R_{eq} values were then plotted *versus* the total protein concentration ($[P]_o$), and K_d values were determined by nonlinear least squares analysis of the binding isotherm using the equation $R_{eq} = R_{max}/(1 + K_d/[P]_o)$.

Crystallization of $ExoU_{P.flu}$—Crystallization of $ExoU_{P.\ flu}$ was performed at a protein concentration of 5.8 mg/ml in 10 mM Tris-HCl (pH 8.3) buffer containing 500 mM NaCl and 5 mM 2-mercaptoethanol by the sitting-drop vapor diffusion method at 295 K. Crystals suitable for data collection were obtained from the Classics II Suite (Qiagen Inc., Valencia, CA) condition consisting of 0.2 M ammonium acetate, 25% (w/v) PEG 3350 in 0.1 M BisTris (pH 5.5/6.5) buffer. Crystals were soaked in the well/crystallization solutions for cryoprotection and flash-frozen in liquid nitrogen for x-ray data collection.

TABLE 4
Data collection and structure-refinement statistics
Values in parentheses are for the highest resolution shell.

Data collection	
Space group	$P2_1$
Cell dimensions	
a, *b*, *c* (Å)	67.2, 115.3, 88.4
β (°)	102.8
No. of reflections	43,226 (1,696)
Resolution (Å)	30.00-2.50 (2.54-2.50)
R_{merge} (%)[a]	7.0 (44.1)
I/σ	15.7 (2.1)
Completeness (%)	95.2 (75.7)
Average redundancy	3.7 (2.9)
Refinement	
Resolution (Å)	29.86-2.50 (2.56-2.50)
Completeness (%)	94.8 (74.1)
No. of reflections	41,015 (2,344)
R_{work}[b]/R_{free}[c] (%)	20.6/26.9 (32.4/42.1)
No. of atoms	
Protein (chain A/B)	4,060/3,895
Water (oxygen atoms)	207
B-factor (Å^2)	
Overall	56.7
Protein (chain A/B)	47.9/66.5
Water	47.5
Coordinate deviation	
r.m.s.d.[e] bond lengths (Å)	0.014
r.m.s.d. bond angles (°)	1.609
Ramachandran statistics[d]	
Most favorite (%)	94.6
Allowed (%)	5.0
Generously allowed (%)	0.5
Outside allowed (%)	0.0

[a] $R_{merge} = \Sigma_{hkl}|I - \langle I\rangle|/\Sigma_{hkl}I$.
[b] $R_{work} = \Sigma|F_{obs} - F_{calc}|/\Sigma|F_{obs}|$, where F_{obs} and F_{calc} are the observed and the calculated structure factors, respectively.
[c] R_{free} were calculated using 5% of total reflections randomly chosen and excluded from the refinement.
[d] Statistics are based on PROCHECK (17).
[e] r.m.s.d. is root mean square deviation.

Data Collection and Structure Determination—A single-wavelength (λ = 0.97856) oscillation x-ray data set was collected on the Life Science Collaborative Access Team (LS-CAT) 21-ID-G. Diffraction images were indexed and scaled with *HKL*-2000 (41) to 2.5 Å resolution. Cell content analysis indicated the presence of two molecules of $ExoU_{P.\ flu}$ (V_m (Matthews coefficient) = 2.4; *versus* (solvent content) = 49.5%) within the $P2_1$ space group at 2.5 Å resolution. A partial molecular replacement solution of $ExoU_{P.\ flu}$ was obtained running Phaser (42) from the CCP4 package (43) and the $ExoU_{P.\ aer}$ structure (Protein Data Bank 3TU3 (28)) as a search model. The structure solution was rebuilt, and water molecules were added using ARP/wARP (44) from the CCP4 package. The structure was refined with REFMAC version 5.7 (45) from the CCP4 package with further manual building and alteration in Coot (46, 47). The quality of the structure was checked with the Protein Data Bank validation server (ADIT validation server) and MolProbity (48, 49). Total buried surface area of the $ExoU_{P.\ flu}$ dimer was determined by the "Protein interfaces, surfaces, and assemblies" service PISA at the European Bioinformatics Institute (50). Structure figures were generated with PyMOL (51). Data collection and structure-refinement statistics are given in Table 4. The final model was deposited in the Protein Data Bank under accession code 4QMK. Diffraction images for the deposited structure are available at the Center for Structural Genomics of Infectious Diseases (CSGID) website.

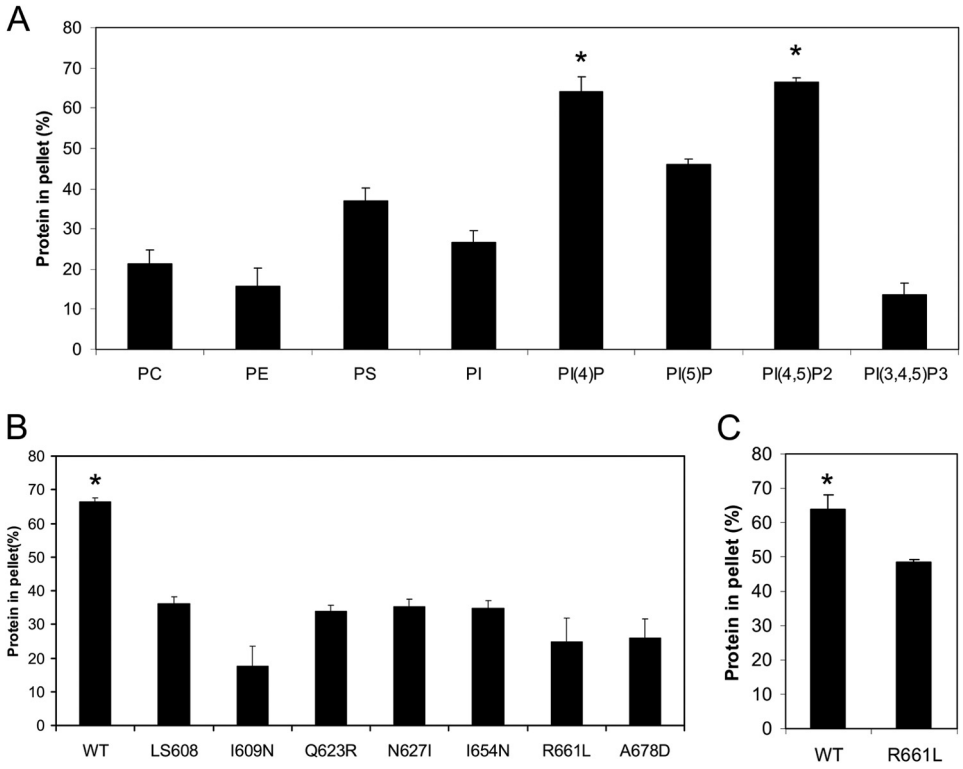

FIGURE 1. **ExoU MLD requires specific residues to bind to PI(4,5)P_2.** *A,* recombinant ExoU MLD (residues 503–687) was tested for co-sedimentation in liposome binding assays with various lipids. Liposomes consisting of 30% PC, 20% PE, and 20% cholesterol were supplemented with 30% of the indicated lipids, except for PI(4)P, PI(5)P, PI(4,5)P_2, and PI(3,4,5)P_3, for which 5% was added (the remaining 25% was PC). Each assay was performed at least in triplicate; values are means, and *error bars* represent S.E. *, $p < 0.05$ compared with all other groups. The difference between PI(4)P and PI(4,5)P_2 is not significant. *PI,* phosphatidylinositol. *B,* recombinant MLD proteins containing single amino acid substitutions (I609N, Q623R, N627I, I654N, R661L, and A678D) or a 5-amino acid insertion (LS608) were tested for binding to PI(4,5)P_2-containing liposomes in co-sedimentation assays. Each assay was performed at least in triplicate; values are means, and *error bars* represent S.E. WT indicates the wild-type MLD of ExoU, using the PI(4,5)P_2 binding data depicted in *A*. *, $p < 0.001$ compared with each variant. No difference between the variants is statistically significant. *C,* recombinant wild-type (*WT*) and R661L MLD protein were analyzed for binding to PI(4)P-containing liposomes. *, $p < 0.05$ relative to R661L variant.

Statistical Methods—Student's *t* test was used to compare means for cytotoxicity assays and yeast viability experiments. Significance was defined as a *p* value of <0.05. One-way analysis of variance was used for all other assays with multiple comparisons with the Bonferroni multiple comparisons test to determine significance.

RESULTS

MLD of ExoU Binds to PI(4,5)P_2—We sought to determine whether ExoU localization to the plasma membrane was mediated by direct affinity to phospholipids, as has been reported for several other toxins (8, 38). Although ExoU was known to bind to PI(4,5)P_2, it was unclear whether this was required for localization or whether the MLD of ExoU was sufficient to mediate this binding (32). To investigate this, we purified the recombinant MLD of ExoU (residues 503–687) and tested it for co-sedimentation with neutral liposomes supplemented with various phospholipids (38, 52). We used a final lipid concentration of 3 mM, which has previously been used to effectively assess lipid-protein interactions (38, 52). We found that liposomes supplemented with either PI(4,5)P_2 or PI(4)P bound to ExoU substantially more than other tested lipids (Fig. 1*A*). ExoU binding to PI(4,5)P_2 is consistent with its plasma membrane targeting, as PI(4,5)P_2 is found specifically in the plasma membrane of eukaryotic cells (27, 53). In contrast, PI(4)P is enriched in the Golgi, although a subpopulation of PI(4)P is in the plasma membrane and may contribute to plasma membrane targeting of some proteins (54). These findings are consistent with ExoU binding to PI(4,5)P_2 (and potentially PI(4)P) to achieve plasma membrane localization.

To obtain a more quantitative measure of ExoU lipid binding, we performed surface plasmon resonance (SPR) binding analysis using full-length recombinant ExoU protein and liposomes supported on a solid sensor surface (55). ExoU did not appreciably bind to phosphatidylcholine liposomes but did bind with high affinity to PI(4,5)P_2 liposomes (K_d 110 ± 30 nM; Fig. 2*A*). ExoU also bound to PI(4)P but with lower affinity (K_d 290 ± 30 nM; Fig. 2*B*). These data confirm the liposome co-sedimentation assay results and demonstrate high affinity interactions between ExoU and PI(4,5)P_2 and somewhat weaker interactions between ExoU and PI(4)P, which was not known previously. Liposome binding and SPR assays are more physiological methods of measuring protein-lipid binding than the lipid strips used previously by Gendrin *et al.* (56), potentially explaining why they did not observe ExoU-PI(4)P binding (31). Interestingly, although not required for PI(4,5)P_2 binding, the presence of phosphatidylserine significantly increased ExoU-PI(4,5)P_2 affinity (Fig. 2*C*). The addition of PS mimics its presence at the inner leaflet of the plasma membrane; this phospholipid contributes to the plasma membrane-targeting specificity of other phosphoinositide binding domains (57).

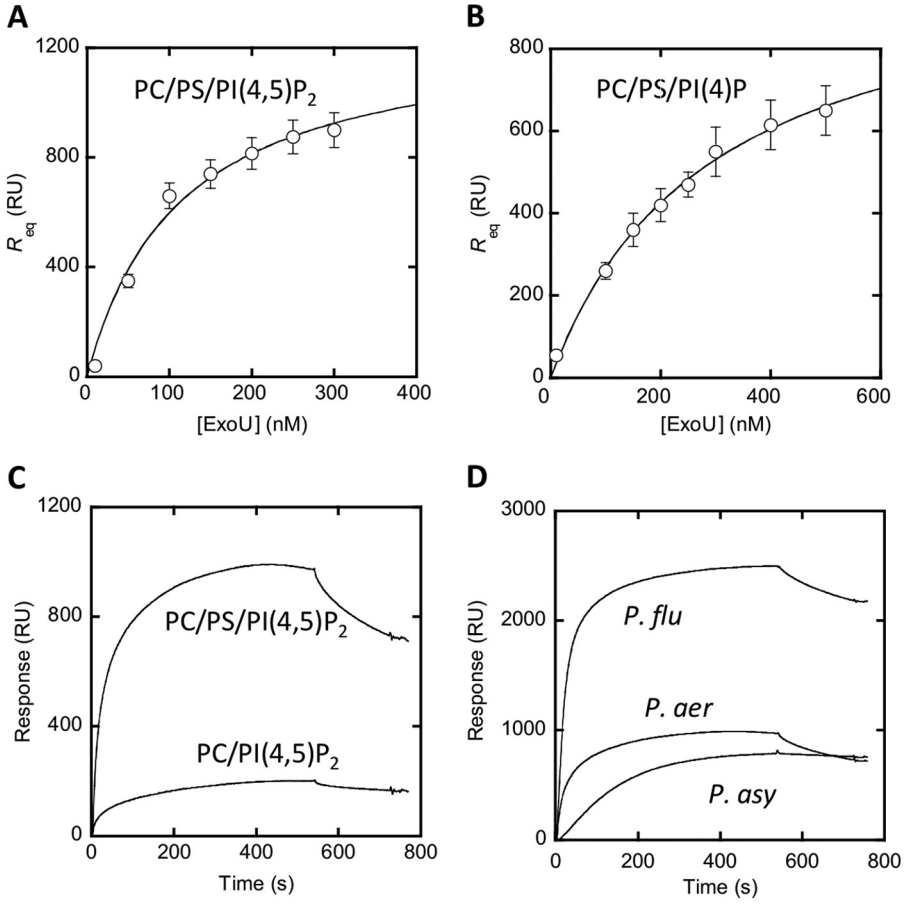

FIGURE 2. **Binding of ExoU to vesicles containing PI(4,5)P_2 and PI(4)P measured by SPR analysis.** *A,* determination of K_d for ExoU binding to PC/PS/PI(4,5)P_2 (77:20:3) vesicles by equilibrium SPR analysis. The binding isotherm was generated from the R_{eq} (average of triplicate measurements) *versus* the concentration (P_0) of ExoU plot. A *solid line* represents a theoretical curve constructed from R_{max} (= 1300 ± 120) and K_d (= 110 ± 30 nM) values determined by nonlinear least squares analysis of the isotherm using the following equation: $R_{eq} = R_{max}/(1 + K_d/P_0)$. *B,* determination of K_d values for ExoU binding to PC/PS/PI(4)P (77:20:3) vesicles by equilibrium SPR analysis. R_{max} (= 1100 ± 60) and K_d (= 290 ± 30 nM) values were calculated as described for *B*. *C,* kinetic SPR sensorgrams for $ExoU_{P.\ aer}$ binding to PC/PS/PI(4,5)P_2 (77:20:3) and PC/PI(4,5)P_2 (97:3) vesicles. *D,* kinetic SPR sensorgrams for $ExoU_{P.\ aer}$, $ExoU_{P.\ flu}$, and $ExoU_{P.\ asy}$ binding to PC/PS/PI(4,5)P_2 (77:20:3) vesicles. $ExoU_{P.\ flu}$ showed the highest degree of vesicle binding. Equilibrium SPR analysis confirmed that it has the highest affinity (K_d = 30 ± 6 nM). *RU*, resonance units. *Error bars* represent S.D.

In an earlier study, we had identified several residues of the MLD that were critical for the proper intracellular localization of ExoU but that did not disrupt the overall secondary structure of ExoU, as measured by circular dichroism (30). We reasoned that if MLD binding to PI(4,5)P_2 truly was responsible for MLD localization to the plasma membrane, then these mislocalized ExoU variants should fail to bind PI(4,5)P_2. We therefore purified recombinant MLD proteins with one of six single amino acid substitutions or with one five-amino acid insertion that had resulted in mislocalization inside host cells (30). These purified proteins were tested for their ability to bind liposomes containing PI(4,5)P_2. Each was deficient in PI(4,5)P_2 binding (Fig. 1*B*), demonstrating that ExoU residues necessary for localization to the plasma membrane of host cells were also critical for binding to PI(4,5)P_2. One variant, R661L, was also tested for binding to PI(4)P. As was the case with PI(4,5)P_2, it was deficient in PI(4)P binding, suggesting that the same mechanism may be used to bind both phosphoinositides (Fig. 1*C*).

ExoU-like MLDs from Other Patatin-like Proteins Also Bind to PI(4,5)P_2—PI(4,5)P_2 binding domains play important roles in intracellular trafficking of eukaryotic proteins, and each distinct binding domain is often utilized by a number of different proteins (33). For this reason, we sought to determine whether other bacterial proteins also used an ExoU MLD-like motif to bind PI(4,5)P_2. Accordingly, BLAST analysis with the MLD of ExoU was used to identify several proteins containing similar MLD sequences (Fig. 3*A*). Genes encoding these proteins were found in the genomes of other *Pseudomonas* species such as *P. fluorescens* and *Pseudomonas syringae* but also in other genera, including *Photorhabdus asymbiotica* and *Burkholderia thailandensis.* Alignments revealed that a number of residues within these sequences were 100% conserved among this group of proteins, including some residues that had previously been shown to be important for ExoU localization, such as Gln-623, Asn-627, Arg-661, and Ala-678 (Fig. 3*A*) (30). Of special interest was Arg-661 of ExoU, a highly conserved and positively charged residue in a loop at the exposed cap of the four-helical bundle in the MLD (28). This residue could potentially directly interact with the negatively charged phosphate groups of PI(4,5)P_2. In support of this model, substitution of Arg-661 with a leucine (R661L) had previously been shown to cause loss of activation of *P. aeruginosa* ExoU by PI(4,5)P_2 (26). Likewise, recombinant MLD protein with this substitution did not bind

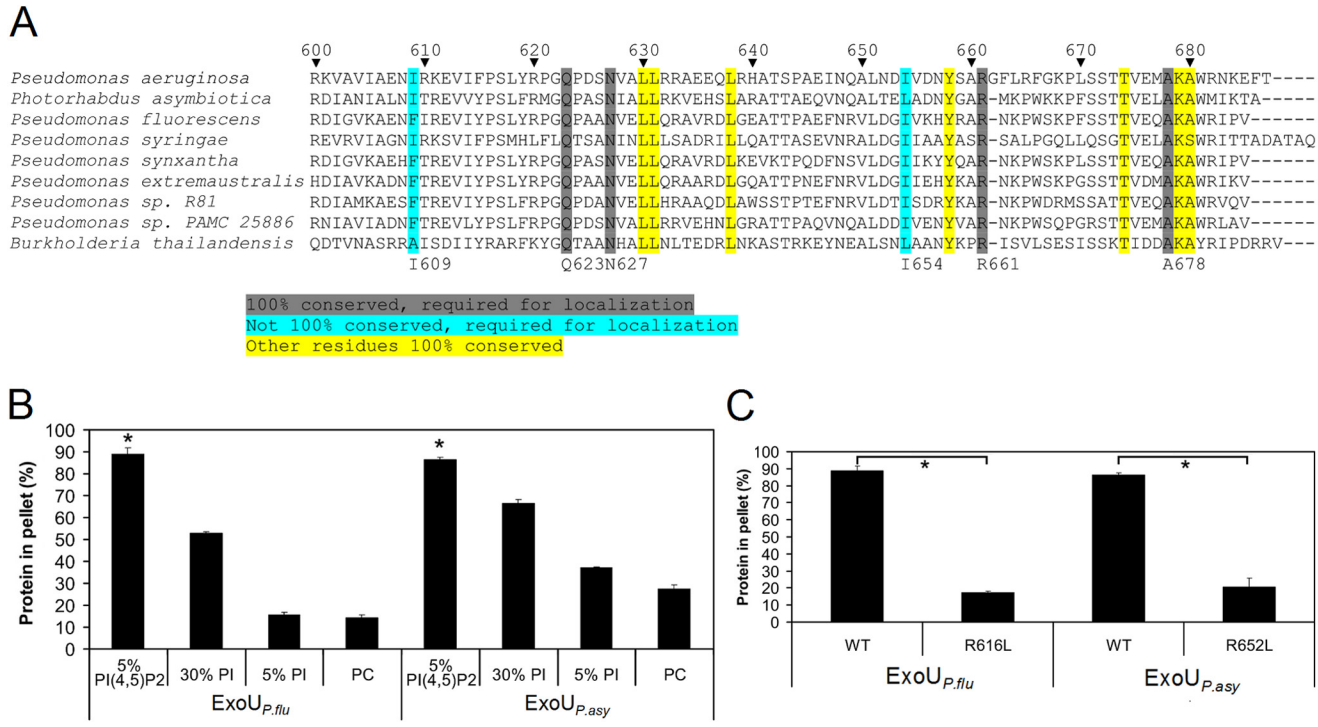

FIGURE 3. **Several residues necessary for the binding of ExoU to PI(4,5)P_2 are conserved in other proteins containing ExoU MLD-like domains.** *A,* alignments of proteins containing ExoU MLD-like domains. The *highlighted sequences* identify highly conserved residues. Those residues highlighted in *gray* and *blue* were critical for ExoU localization in mammalian cells (30) and for binding to PI(4,5)P_2-supplemented liposomes (Fig. 1*B*). Numbering system refers to ExoU of *P. aeruginosa*. Accession numbers for the indicated proteins in order are as follows: O34208, YP_003039880.1, YP_006326405.1, ZP_07262921.1, ZP_10142741.1, ZP_10438440.1, ZP_11185695.1, ZP_10426928.1, and ZP_18329767.1. *B,* recombinant putative MLD proteins from $ExoU_{P.\ flu}$ and $ExoU_{P.\ asy}$ (residues 453–639 and 495–676, respectively) were purified and assayed for liposome binding. Liposomes consisted of the same composition as depicted in Fig. 1, except that 5% PI/25% PC-supplemented liposomes were also tested. *C,* arginine-to-leucine substitutions corresponding to R661L in $ExoU_{P.\ aer}$ were generated in $ExoU_{P.\ flu}$ and $ExoU_{P.\ asy}$ recombinant MLD proteins. These proteins were purified and were tested for binding to liposomes supplemented with 5% PI(4,5)P_2. The results for "WT," which refers to wild-type protein, are the same as depicted in *B*. Each assay was performed in triplicate; values are means, and *error bars* represent S.E. *, $p < 0.001$ for PI(4,5)P_2 compared with other lipids and wild-type compared with arginine-to-leucine substitution proteins.

PI(4,5)P_2 in liposome binding assays (Fig. 1*B*). These results suggest that this conserved arginine residue might be critical for direct MLD binding to PI(4,5)P_2.

To investigate whether ExoU MLD-like domains from other bacteria also bound PI(4,5)P_2, we tested the recombinant MLDs from *P. fluorescens* and *P. asymbiotica* in the liposome binding assay. *P. fluorescens* is an environmental bacterium (58), and *P. asymbiotica* infects insects and is an emerging human pathogen (59). The MLD-containing proteins from these bacteria had not been previously studied (59, 60), but their homologies to ExoU extended beyond the MLDs. For this reason, we will refer to them as $ExoU_{P.\ flu}$ and $ExoU_{P.\ asy}$, respectively. We found that the recombinant MLD proteins from $ExoU_{P.\ flu}$ and $ExoU_{P.\ asy}$ bound to PI(4,5)P_2 significantly more than to phosphatidylcholine (Fig. 3*B*). Each protein also bound to phosphatidylinositol, albeit to a lesser degree than to PI(4,5)P_2. These results were recapitulated with SPR analysis, which found that $ExoU_{P.\ flu}$ bound to PI(4,5)P_2 with high affinity ($K_d = 30 \pm 6$ nM) (Fig. 2*D*). SPR also detected $ExoU_{P.\ asy}$ binding to PI(4,5)P_2, but this binding was of lower affinity (K_d value not calculated).

We then investigated whether substitution of the conserved arginine residue corresponding to Arg-661 in $ExoU_{P.\ aer}$ altered the ability of these homologs to bind PI(4,5)P_2. Indeed, $ExoU_{P.\ flu}$-R616L and $ExoU_{P.\ asy}$-R652L were each substantially reduced in PI(4,5)P_2 binding compared with their wild-type counterparts (Fig. 3*C*). These results indicate that the MLD of ExoU represents a new PI(4,5)P_2 binding domain used by multiple bacterial species and that a conserved arginine residue is important for this binding.

ExoU and Other Patatin-like Proteins Localize in a PI(4,5)P_2-dependent Manner—Having characterized the *in vitro* PI(4,5)P_2 binding of the MLDs of several ExoU proteins, we sought to determine whether this binding contributed to localization. To this end, the intracellular localization of the MLD of each of the *P. aeruginosa*, *P. fluorescens*, and *P. asymbiotica* proteins was investigated by transfection of HeLa cells with constructs expressing GFP-tagged MLD proteins. Consistent with their ability to bind PI(4,5)P_2 *in vitro*, each of the MLD proteins localized to the plasma membrane (Fig. 4, *A*, *C,* and *E*). As demonstrated previously, the R661L substitution in the $ExoU_{P.\ aer}$ MLD abolished membrane localization, with the protein becoming diffusely localized (Fig. 4*B*) (30). Similar results were observed with the corresponding R616L substitution in $ExoU_{P.\ flu}$ and the R652L substitution in $ExoU_{P.\ asy}$, although the latter protein was associated with a less homogeneous intracellular distribution (Fig. 4, *D* and *F*). Overall, these results indicate that loss of PI(4,5)P_2 binding *in vitro* is correlated with decreased localization to the plasma membrane and demonstrate the importance of the conserved MLD arginine residue to this process.

To solidify the importance of PI(4,5)P_2 in mediating targeting of ExoU to the plasma membrane, we used a yeast model

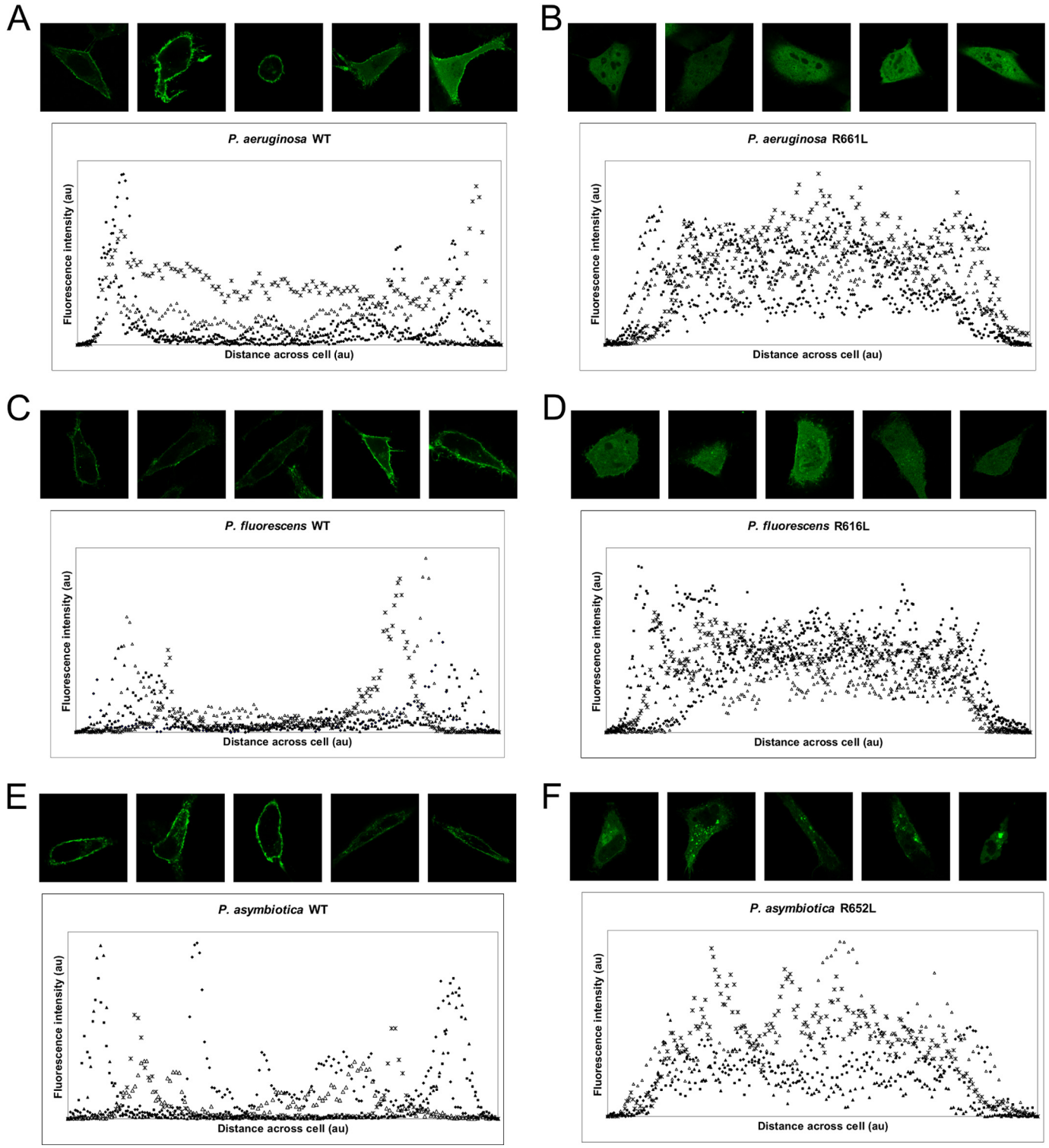

FIGURE 4. **MLDs from ExoU$_{P.\ aer}$, ExoU$_{P.\ flu}$, and ExoU$_{P.\ asy}$ localize to the plasma membrane of HeLa cells.** HeLa cells were transfected with constructs expressing GFP-tagged MLD proteins from the ExoU homologs of *P. aeruginosa*, *P. fluorescens*, and *P. asymbiotica*. Representative images were visualized by fluorescence microscopy. Both wild-type (*WT*) (*A*, *C*, and *E*) and arginine-to-leucine substitutions (*B*, *D*, and *F*) of each protein were tested. Images were analyzed for fluorescence intensity distribution across cells using ImageJ. The distance and fluorescence intensity are in arbitrary units (*au*).

that was amenable to manipulation of PI(4,5)P_2 localization. Yeast are an established model system for the study of ExoU activity and localization and have yielded results similar to those observed in mammalian cells (26, 37). We reasoned that if ExoU localization was truly dependent on binding to PI(4,5)P_2, then mislocalization of PI(4,5)P_2 should cause a corresponding mislocalization of ExoU. In these experiments, PI(4,5)P_2 was visualized in yeast using a construct that expressed a GFP-tagged pleckstrin homology (PH) domain from mammalian phospholipase Cδ, which is a natural ligand of PI(4,5)P_2 (Fig.

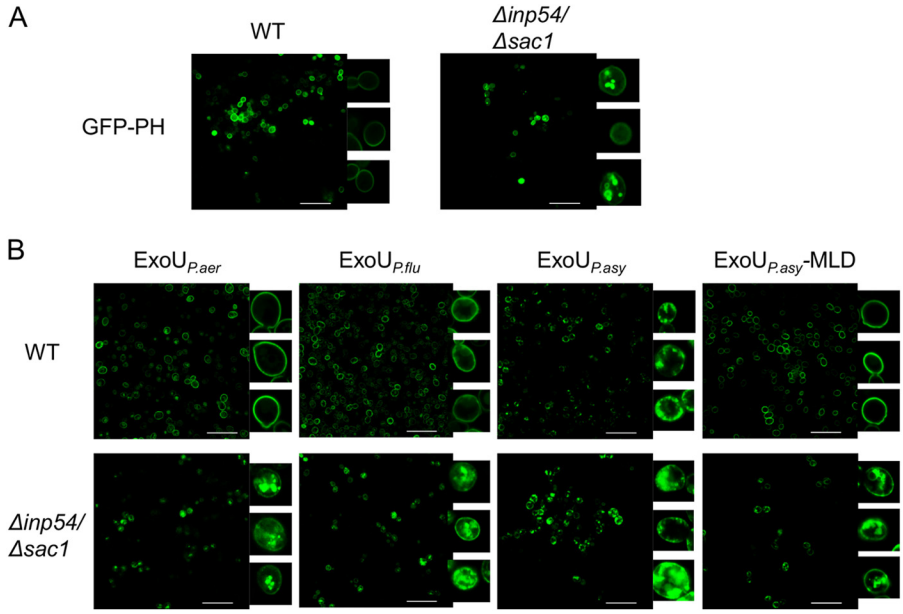

FIGURE 5. **ExoU$_{P.\ aer}$, ExoU$_{P.\ flu}$, and ExoU$_{P.\ asy}$ localize to the plasma membrane of yeast in a PI(4,5)P$_2$-dependent fashion.** *A,* PI(4,5)P$_2$ localization was visualized in wild-type (*WT*) and Δ*inp54*/Δ*sac1* yeast by the expression of GFP-tagged pleckstrin homology domain from phospholipase C. Yeast were visualized using fluorescence confocal microscopy. *B,* GFP-tagged catalytically inactive ExoU proteins were visualized by fluorescence confocal microscopy following expression in yeast. The *insets* show individual yeast cells magnified ×15. ExoU$_{P.\ asy}$-MLD refers to the membrane localization domain of ExoU$_{P.\ asy}$ *Scale bars,* 25 μm.

5*A*) (61). In wild-type yeast, PI(4,5)P$_2$ exhibited a peripheral distribution, consistent with plasma membrane localization. However, in a Δ*inp54*/Δ*sac1* yeast mutant, which lacks two phosphatases important for appropriate PI(4,5)P$_2$ distribution, this phospholipid was mislocalized to the vacuole and cytosol (Fig. 5*A*), as described previously (61). Prior reports demonstrated that PI(4)P localization is unchanged in these yeast and that proteins that localize to the plasma membrane independently of PI(4,5)P$_2$ are also unaffected (61). Full-length ExoU$_{P.\ aer}$ tagged with GFP localized to the plasma membrane in wild-type yeast but was largely associated with intracellular structures in Δ*inp54*/Δ*sac1* mutant yeast (Fig. 5*B*). Thus, mislocalization of PI(4,5)P$_2$ resulted in a similar mislocalization of ExoU$_{P.\ aer}$, consistent with the model that ExoU$_{P.\ aer}$ binds to PI(4,5)P$_2$ to target the plasma membrane.

We next assessed the localization of ExoU$_{P.\ flu}$ and ExoU$_{P.\ asy}$ in yeast. In wild-type yeast, full-length ExoU$_{P.\ flu}$ localized to the plasma membrane similarly to ExoU$_{P.\ aer}$ (Fig. 5*B*). In the Δ*inp54*/Δ*sac1* mutant yeast, ExoU$_{P.\ flu}$ displayed mislocalization away from the plasma membrane, indicating PI(4,5)P$_2$-dependent localization. ExoU$_{P.\ asy}$ also localized to the plasma membrane in wild-type yeast but formed more punctate structures at or adjacent to the membrane (Fig. 5*B*). In the Δ*inp54*/Δ*sac1* mutant yeast, the distribution of ExoU$_{P.\ asy}$ shifted somewhat to the interior of the yeast, although substantial amounts remained at the periphery. Because the localization of full-length ExoU$_{P.\ asy}$ in yeast differed from that of the ExoU$_{P.\ asy}$ MLD in HeLa cells, we examined the localization of the ExoU$_{P.\ asy}$ MLD in yeast. As observed in HeLa cells, the MLD alone localized specifically to the plasma membrane of yeast (Fig. 5*B*). Importantly, the ExoU$_{P.\ asy}$ MLD was mislocalized in Δ*inp54*/Δ*sac1* yeast, suggesting that localization of the ExoU$_{P.\ asy}$ MLD is dependent on PI(4,5)P$_2$. These results suggest that the MLD of ExoU$_{P.\ asy}$ requires PI(4,5)P$_2$ for localization but that full-length ExoU$_{P.\ asy}$ may have residues outside the MLD that contribute to an altered intracellular distribution. Together these data indicate that ExoU and its homologs localize to the plasma membrane in a PI(4,5)P$_2$-dependent manner, either as full-length proteins or as isolated MLD domains.

ExoU$_{P.\ flu}$ and ExoU$_{P.\ asy}$ Are Also Phospholipases—The proteins listed in Fig. 3*A* contained regions with similarity to not only the MLD of ExoU$_{P.\ aer}$ but also to its catalytic domain. In particular, both ExoU$_{P.\ flu}$ and ExoU$_{P.\ asy}$ have a putative PLA$_2$ serine-aspartate catalytic dyad and glycine-rich oxyanion hole characteristic of patatin-like phospholipases (Fig. 6*A*). We therefore examined whether these proteins have PLA$_2$ activity. We first confirmed that ExoU$_{P.\ aer}$ by itself does not have PLA$_2$ activity but is synergistically activated by a combination of ubiquitin and PI(4,5)P$_2$ (Fig. 6*B*) (25, 26). To test whether ExoU$_{P.\ flu}$ and ExoU$_{P.\ asy}$ act as phospholipases, recombinant versions of both proteins were purified and assessed *in vitro* for evidence of PLA$_2$ activity. The enzymatic characteristics of ExoU$_{P.\ asy}$ were similar to those of ExoU$_{P.\ aer}$, with no activity on its own and a synergistic activation with the addition of ubiquitin and PI(4,5)P$_2$ (Fig. 6*B*). However, the overall activity of ExoU$_{P.\ asy}$ when combined with ubiquitin and PI(4,5)P$_2$ was low, only 22% that of ExoU$_{P.\ aer}$ under the conditions of these assays. In contrast, ExoU$_{P.\ flu}$ alone had considerable PLA$_2$ activity, and the addition of ubiquitin substantially increased this activity (Fig. 6*B*). In fact, addition of only 0.1% as much ubiquitin as ExoU$_{P.\ flu}$ resulted in significantly increased PLA$_2$ activity. Supplementation with PI(4,5)P$_2$, however, caused only a slight additional increase in catalytic activity, suggesting that ubiquitin plays a more predominant role in the activation of ExoU$_{P.\ flu}$. These results demonstrate that MLD-containing patatin-like proteins from other bacterial species and genera also have PLA$_2$ activity but differ

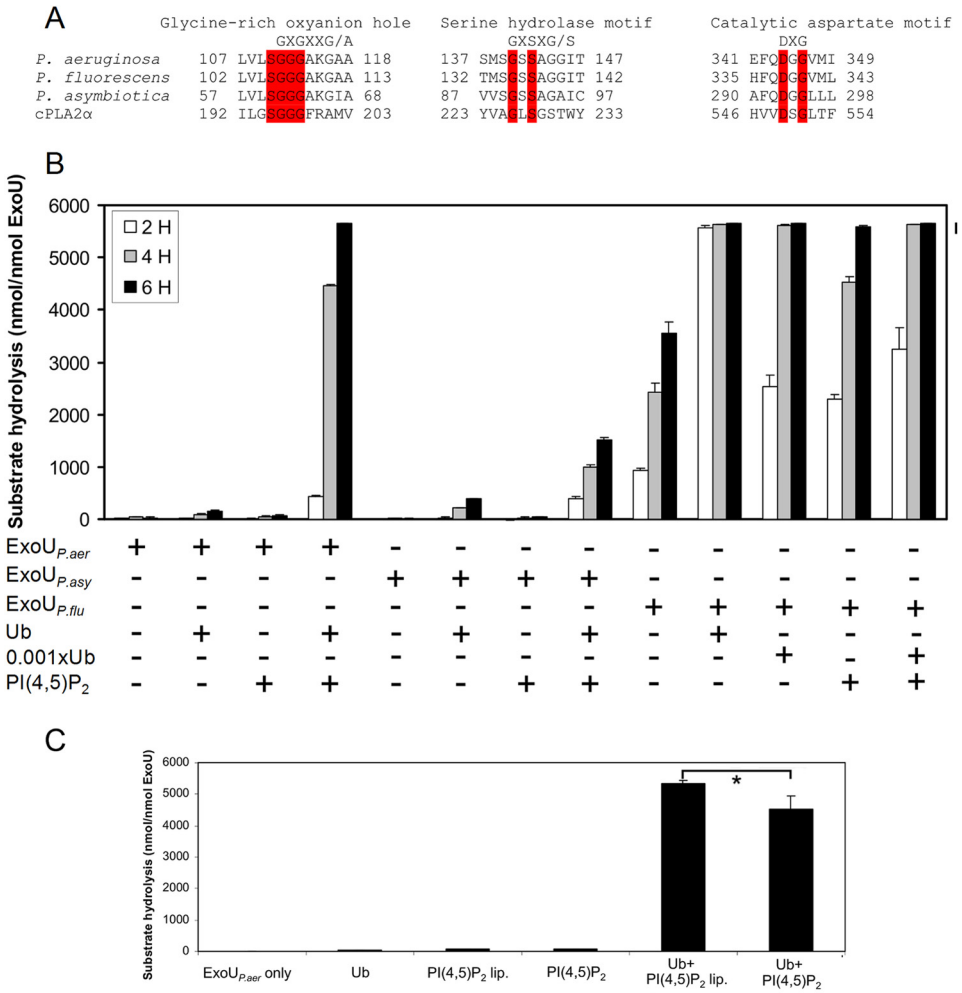

FIGURE 6. **ExoU$_{P.\ flu}$ and ExoU$_{P.\ asy}$ have PLA$_2$ activity.** *A,* ExoU$_{P.\ aer}$ and its homologs from *P. fluorescens* and *P. asymbiotica* were aligned with cPLA$_2$ (accession number P47712.2) at their putative catalytic sites. Residues highlighted in *red* are identical in each of these proteins. *B,* PLA$_2$ activity of each of these proteins was measured *in vitro* using a synthetic phospholipid substrate. Each protein was analyzed for its ability to hydrolyze substrate by itself, with ubiquitin, with PI(4,5)P$_2$, or with both ubiquitin and PI(4,5)P$_2$. Ubiquitin (*Ub*) was added at a 1:1 ubiquitin/ExoU molar ratio or at a 1:1000 ratio (*0.001*×*Ub*). *C,* PLA$_2$ activity of ExoU$_{P.\ aer}$ was measured with the addition of ubiquitin, PI(4,5)P$_2$, or PI(4,5)P$_2$-containing liposomes with the same overall PI(4,5)P$_2$ concentration (*PI(4,5)P$_2$ lip.*). PLA$_2$ activity was measured at 5 h. Each assay was performed in triplicate; values are means, and *error bars* are S.E. *, $p < 0.01$.

from ExoU$_{P.\ aer}$ in how active they are by themselves or with ubiquitin and PI(4,5)P$_2$. ExoU$_{P.\ aer}$ was also activated by PI(4,5)P$_2$-containing liposomes, indicating that the liposome binding assay conditions are suitable for ExoU activation in the presence of ubiquitin (Fig. 6*C*).

We next examined whether ExoU$_{P.\ flu}$ and ExoU$_{P.\ asy}$, like ExoU$_{P.\ aer}$, could kill eukaryotic cells. Each of these proteins was expressed in HeLa cells by transfection, and cytotoxicity was assessed by measuring lactate dehydrogenase release. ExoU$_{P.\ aer}$, as shown previously, caused substantial cytotoxicity by 24 h, and this cytotoxicity was diminished by substituting an alanine for the catalytic serine at position 142 within the PLA$_2$ domain (Fig. 7*A*) (30). Consistent with its high PLA$_2$ activity, ExoU$_{P.\ flu}$ was also highly cytotoxic, and substitution of its putative catalytic serine also resulted in decreased cytotoxicity. Because of the rapid lysis of cells following expression of ExoU$_{P.\ aer}$ and ExoU$_{P.\ flu}$, these proteins could not be detected within transfected cells, whereas expression of the proteins with catalytic site substitutions could be detected (Fig. 7*B*). Despite repeated attempts, we were not able to detect stable GFP-tagged protein in cells transfected with ExoU$_{P.\ asy}$-expressing constructs and were therefore unable to assess the cytotoxicity of this protein (Fig. 7*B*). Detection following substitution of other tags in place of GFP was also not successful (data not shown). Interestingly, the MLD of ExoU$_{P.\ asy}$ was stable when expressed by itself in mammalian cells (Fig. 4), and the full-length GFP-tagged ExoU$_{P.\ asy}$-S137A construct could be visualized in yeast (Fig. 5*B*). It is possible that the full-length ExoU$_{P.\ asy}$ protein may not fold properly in the mammalian cell cytosol or it may be destabilized or degraded. Overall, these experiments demonstrated that ExoU$_{P.\ flu}$ is cytotoxic to HeLa cells, but we could not assess the cytotoxicity of ExoU$_{P.\ asy}$ in this cell type.

ExoU$_{P.\ flu}$ Crystal Structure and Its Comparison with the Structure of ExoU$_{P.\ aer}$—As mentioned, the crystal structure of ExoU$_{P.\ aer}$ was recently determined and suggested that the four-helical bundle region of the MLD might bind to the plasma membrane (28, 31), similar to the four-helical bundles of other toxins (8, 29). This structure suffered from two limitations. First, ExoU$_{P.\ aer}$ could only be crystallized in complex with its cognate chaperone SpcU, a bacterial protein that is not present

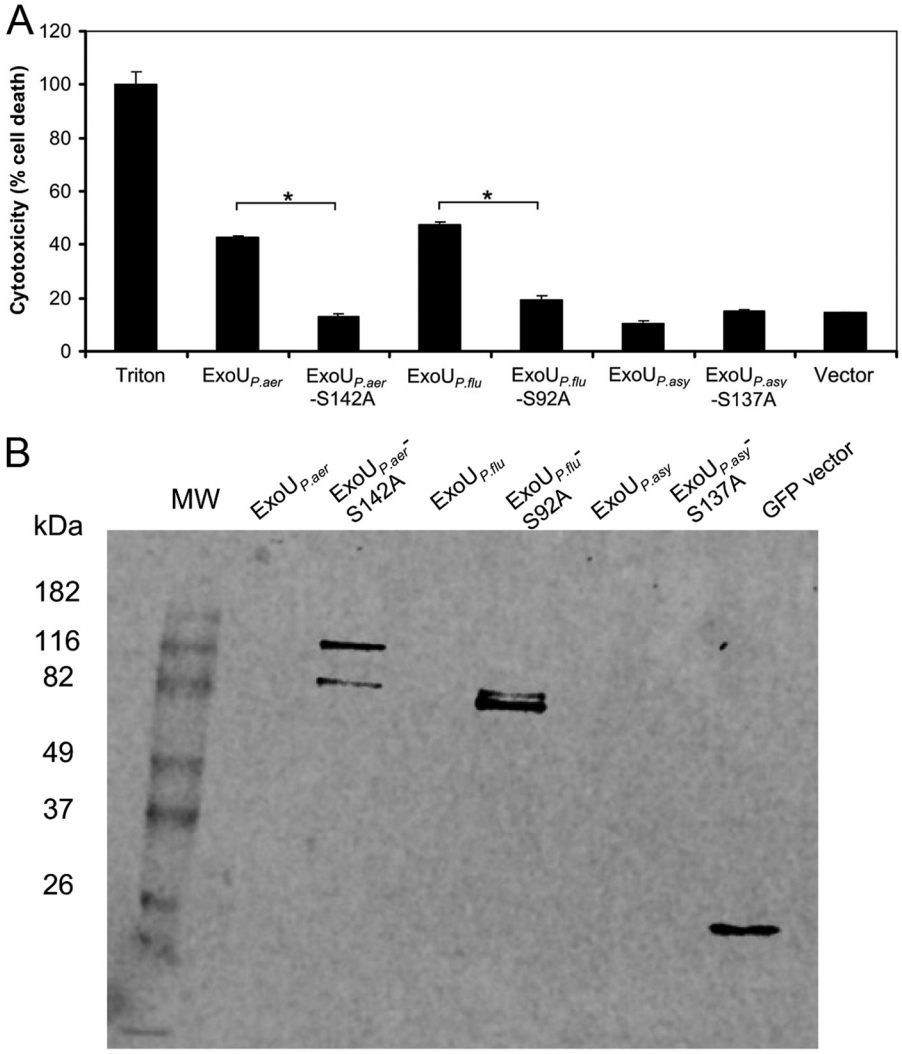

FIGURE 7. **Cytotoxicity of ExoU homologs.** *A,* HeLa cells were transfected with ExoU expression constructs and analyzed for release of lactate dehydrogenase as a measure of cell death. Results were normalized to treatment with Triton X-100 (100% cell death) and mock-transfected cells (0% cell death). *Vector* indicates transfection of pcDNA3.1 NT-GFP vector without insert. Each assay was performed in triplicate; values are means, and *error bars* represent S.E. *, $p < 0.001$. *B,* same GFP-tagged constructs shown in *A* were transfected into HeLa cells, which were subsequently analyzed for expression of the resulting proteins with anti-GFP antibody. *MW* denotes the molecular weight markers.

inside eukaryotic cells. Thus, the relevance of this structure to ExoU$_{P.\ aer}$ interaction with eukaryotic membranes is unclear. Second, the loop containing the conserved Arg-661 was disordered in this structure, preventing an assessment of how it may promote membrane localization. In the hopes of overcoming these limitations and to further investigate MLD-PI(4,5)P_2 interactions, we attempted to crystallize full-length ExoU$_{P.\ flu}$. We successfully crystallized this protein in the absence of any chaperone proteins and determined its structure to 2.5 Å resolution (Fig. 8*A*). Surprisingly, ExoU$_{P.\ flu}$ crystallized as a dimer, with a total buried surface area of ~2000 Å^2 (Fig. 8*B*). Residues 130–169 (helices α4 and α5) of each patatin-like PLA_2 domain constitute the primary interaction interface within the dimer. This dimeric structure is mainly stabilized by stretches of hydrophobic amino acids buried at the interface (Fig. 8*C*).

Comparison with the domain architecture of ExoU$_{P.\ aer}$ (28) allowed the ExoU$_{P.\ flu}$ structure to be broadly divided into four domains as follows: a putative chaperone binding domain (residues 21–51 and 421–451), a patatin-like PLA_2 domain (residues 52–420), and an MLD region, which encompasses domains three and four (residues 452–559 and 560–639, respectively) (Fig. 8*A*). ExoU$_{P.\ aer}$ and ExoU$_{P.\ flu}$ are quite similar in their overall tertiary structures, overlapping with root-mean-square deviation of 2.2 Å (based on the DaliLite server (62–64)) over 473 Cα atoms (Fig. 9). The two ExoU structures also have comparable disordered regions (Fig. 9). The catalytic region of the two proteins are similar as well, with the glycine-rich oxyanion hole (Gly-61–63 in ExoU$_{P.\ flu}$ and Gly-111–113 in ExoU$_{P.\ aer}$) and the serine hydrolase motif containing catalytic Ser-92 (Ser-142 in ExoU$_{P.\ aer}$) each aligning well structurally (Fig. 10*A*) (65). Gly-286, an additional glycine important for ExoU$_{P.\ aer}$ activity, is also conserved structurally (Fig. 10*A*, Gly-235 in ExoU$_{P.\ flu}$) (65). The catalytic Asp-294 was not modeled due to disorder, as was previously the case for ExoU$_{P.\ aer}$ (28). Notably, the chaperone binding domains of these two proteins are less similar, suggesting that ExoU$_{P.\ flu}$ has a structurally distinct chaperone, lacks a chaperone, or that crystal packing has affected the domain's orientation in ExoU$_{P.\ flu}$ (Fig. 9). It is

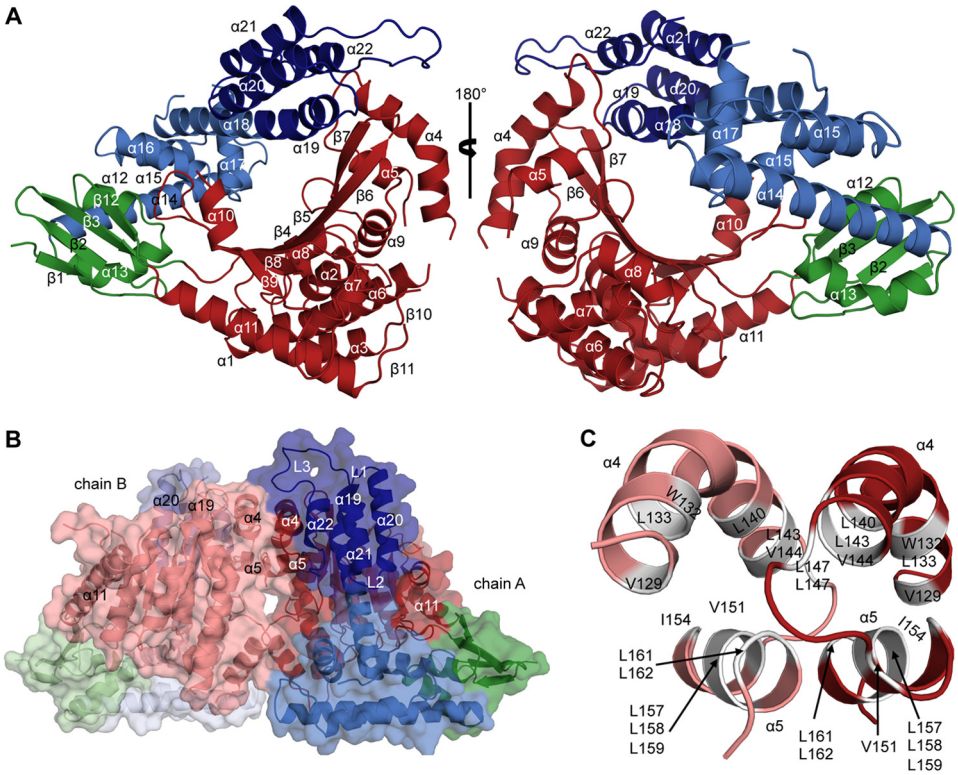

FIGURE 8. **Crystal structure of ExoU from *P. fluorescens*.** *A, ribbon* diagram of a single ExoU$_{P.\ flu}$ molecule showing subunit domain 1 (the putative chaperone binding domain, *green*), domain 2 (the patatin PLA$_2$ domain, *red*), domain 3 (*light blue*), and domain 4 (*dark blue*). Domains 3 and 4 together constitute the MLD. *B,* ribbon and surface representation of the asymmetric unit composition of the structure showing the dimeric arrangement of ExoU$_{P.\ flu}$. L1, L2, and L3 are loops of domain 4 that connect the helices 19–20, 20–21, and 21–22, respectively, of the four-helical bundle. *C,* major dimerization interface generated by helices 4 and 5 of the patatin PLA$_2$ domain. Buried hydrophobic residues (*white* and labeled with *one-letter code*) within the helices are displayed.

unclear whether this may explain potential PLA$_2$ activity differences between the two proteins.

The MLD regions (domains three and four) of ExoU$_{P.\ flu}$ and ExoU$_{P.\ aer}$ are very similar structurally, with domain four of each protein forming a four-helical bundle that overlaps with root-mean-square deviation of just 0.7 Å (Fig. 11*A*). The conserved Arg-616 of ExoU$_{P.\ flu}$ is part of the L3 loop that protrudes from the four-helical bundle, similarly located to Arg-661 of ExoU$_{P.\ aer}$. As mentioned, the conserved nature of this arginine, its location at the cap of the four-helical bundle, its critical role in membrane localization (Fig. 4), and its positive charge makes it an attractive candidate for binding to the negatively charged phosphates of PI(4,5)P$_2$. Whereas the portion of the ExoU$_{P.\ aer}$ L3 loop containing Arg-661 was disordered, this loop was modeled in the ExoU$_{P.\ flu}$ structure (Fig. 11*A*). One of the ExoU$_{P.\ flu}$ monomers showed the L3 loop protruding and well positioned to interact with membranes (Fig. 8*B*). Importantly, the ExoU$_{P.\ flu}$ monomers have both the four-helical bundle and the PLA$_2$ catalytic residues oriented to the same face of the protein (Fig. 8*B*). This arrangement is consistent with the four-helical bundle positioning ExoU at the plasma membrane in an orientation that facilitates placement of substrate membrane phospholipids into the catalytic pocket. The caps of the four-helical bundles of both ExoU$_{P.\ flu}$ and ExoU$_{P.\ aer}$ form positively charged surface-exposed pockets, suggesting potential additional contacts with negatively charged PI(4,5)P$_2$ molecules (Fig. 10*B*). Interestingly, this surface charge distribution differs from structurally similar four-helical bundle domains of other toxins such as *P. multocida* toxin (PMT) and *Clostridium difficile* toxin B (TcdB) that do not have specificity for PI(4,5)P$_2$ (Fig. 10*B*). Additional conserved residues important for the localization of ExoU$_{P.\ aer}$ (30) are also structurally conserved in ExoU$_{P.\ flu}$ (Figs. 3*A* and 11*A*). Furthermore, the conserved polar or charged residues Arg-616, Gln-578, and Asn-582 of ExoU$_{P.\ flu}$ (Arg-661, Gln-623, and Asn-627 in ExoU$_{P.\ aer}$) were all located in the cap of the four-helical bundle, suggesting a role in binding to PI(4,5)P$_2$. In contrast, the conserved hydrophobic residues Phe-564, Ile-609, and Ala-632 of ExoU$_{P.\ flu}$ (Ile-609, Ile-654, and Ala-678 in ExoU$_{P.\ aer}$) were located within the α-helices themselves, signifying a role in maintaining the overall four-helical bundle configuration (Fig. 11*A*). In summary, structural data suggest a model whereby the four-helical bundle structural motif is used by many bacterial proteins to interact with a variety of membranes, but the caps of the four-helical bundles of patatin-like proteins have been "customized" to bind PI(4,5)P$_2$ and target these proteins to the plasma membrane of eukaryotic cells.

DISCUSSION

We describe the mechanism by which three members of the patatin-like phospholipases bind PI(4,5)P$_2$ to localize to the plasma membrane of host cells. Using liposome binding assays, we found that the MLD of ExoU$_{P.\ aer}$ has specific affinity for PI(4,5)P$_2$ and that MLD residues important for plasma membrane localization are also critical for PI(4,5)P$_2$ binding. Although the ability of ExoU to bind PI(4,5)P$_2$ was already known (31, 32), we found that PI(4,5)P$_2$ mislocalization dis-

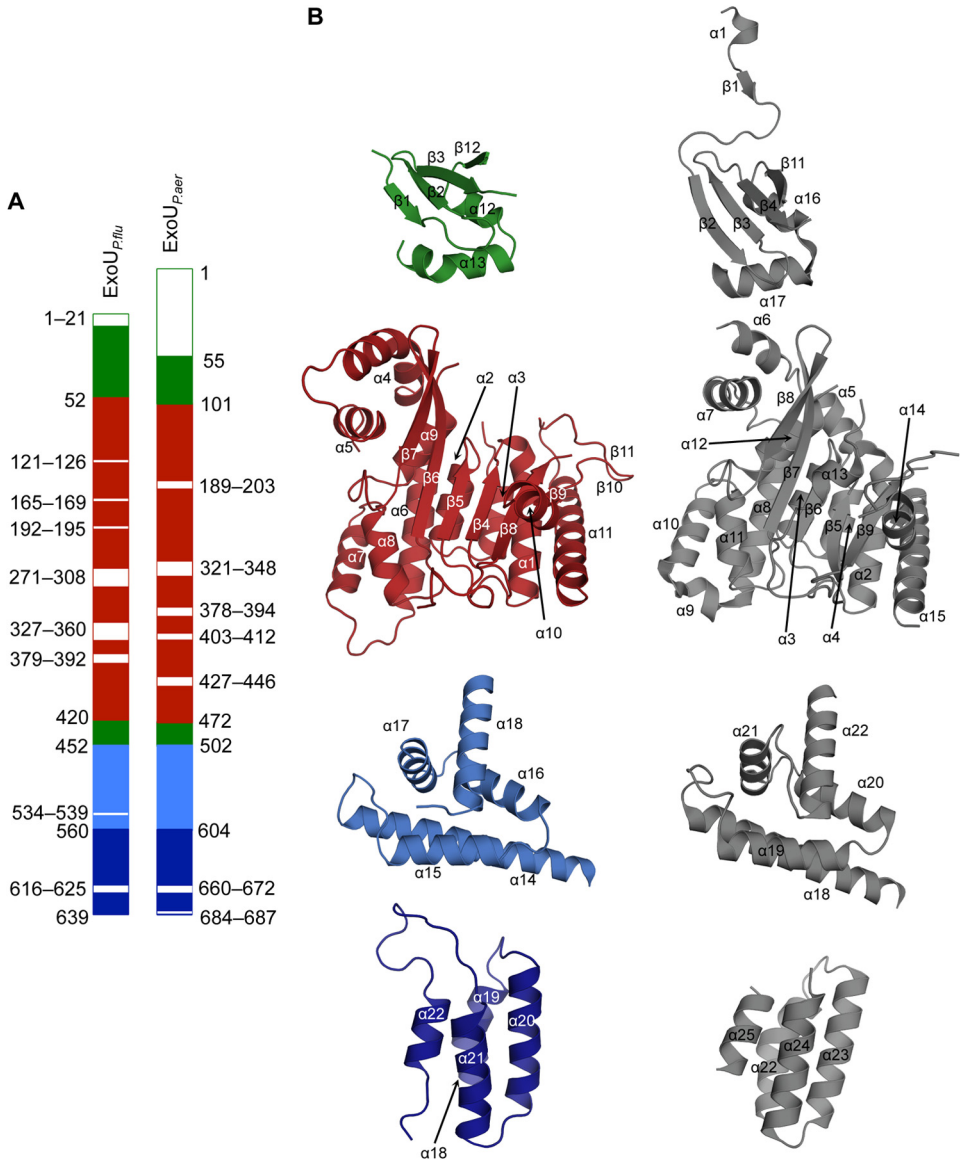

FIGURE 9. **Comparison of the ExoU$_{P. flu}$ and ExoU$_{P. aer}$ structures.** *A,* linear depiction of ExoU$_{P. flu}$ and ExoU$_{P. aer}$ domains. The putative chaperone binding domain (domain 1) is shown in *green*, the patatin PLA_2 domain (domain 2) in *red*, and the MLD in *blue*. The MLD is composed of domain 3 (*light blue*) and domain 4 (*dark blue*). Disordered regions in both structures are shown in *white*. *B,* domain-to-domain comparisons of the least squares superimposed ExoU$_{P. flu}$ (colored as in *A*) and ExoU$_{P. aer}$ (*gray*) structures.

rupted targeting of ExoU$_{P. aer}$ to the plasma membrane. The use of this novel $PI(4,5)P_2$ binding domain is not restricted to ExoU$_{P. aer}$ but was also utilized by patatin-like proteins from *P. fluorescens* and *P. asymbiotica*. The crystal structures of the full-length ExoU$_{P. flu}$ and ExoU$_{P. aer}$ demonstrated that their MLDs likely use a four-helical bundle structural motif to present a positively charged pocket containing a conserved arginine residue important for $PI(4,5)P_2$ binding. Binding of $PI(4,5)P_2$ by this motif may orient the ExoU patatin-like catalytic site toward phospholipid substrates in the plasma membrane. Together, these findings define a new $PI(4,5)P_2$-binding motif used by bacterial proteins to target the plasma membrane of eukaryotic cells, where they are well positioned to access phospholipid substrates within the plasma membrane and to cause cell lysis.

Phosphoinositides (phosphatidylinositol lipids with phosphates attached to the 3-, 4-, or 5-positions of the inositol ring) such as $PI(4,5)P_2$ are critical for the function of eukaryotic cells, often serving as signposts for defined membrane compartments (34). $PI(4,5)P_2$ is predominantly found in the plasma membrane, PI(4)P in the Golgi (66), and PI(3)P in endosomes (67). This allows proteins with particular lipid-binding specificities to be targeted to the corresponding membrane compartments. $PI(4,5)P_2$ binding domains in particular are critical for the function of eukaryotic cells. For example, PH domains, epsin N-terminal homology domains, and FERM domains each target endogenous proteins to the plasma membrane (35, 36, 68). These and other domains play critical roles in cell processes such as endocytosis, motility, and cytoskeletal anchoring (35, 69, 70). They use different mechanisms for $PI(4,5)P_2$ recognition, but a common theme is the presence of basic residues that bind to the negatively charged $PI(4,5)P_2$ (71). Our results add further evidence to the notion that bacteria have evolved mechanisms to co-opt this elaborate localization system.

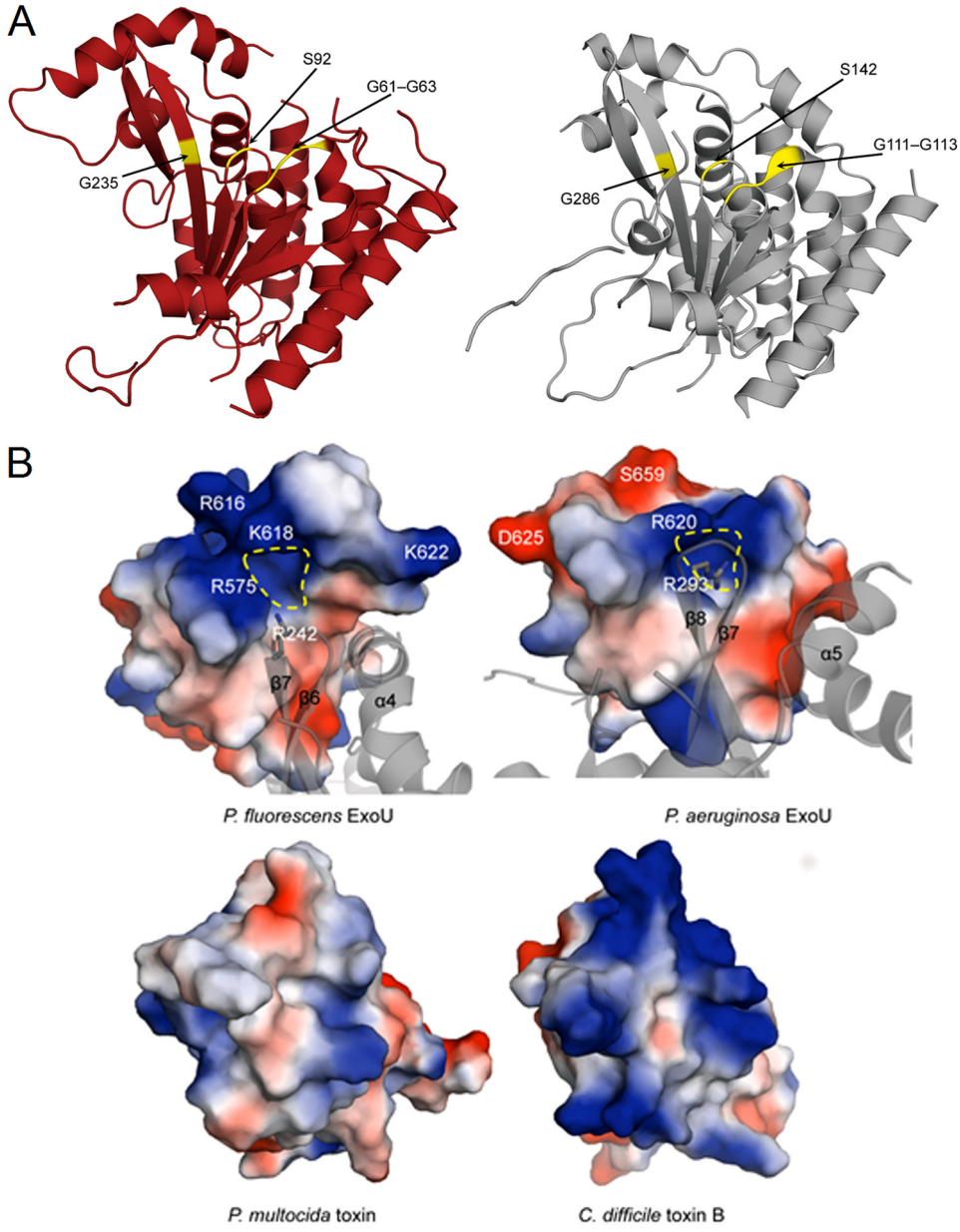

FIGURE 10. **Comparisons of the catalytic regions and surface charge distributions of ExoU proteins.** *A,* comparison of the catalytic patatin PLA_2 domain of $ExoU_{P.\ flu}$ (*red,* chain A used) and $ExoU_{P.\ aer}$ (*silver*). The glycine-rich oxyanion hole region (Gly-61–63 in $ExoU_{P.\ flu}$ and Gly-111–113 in $ExoU_{P.\ aer}$), catalytic serine residue (Ser-92 in $ExoU_{P.\ flu}$ and Ser-142 in $ExoU_{P.\ aer}$), and an additional conserved glycine residue important in activity (Gly-235 in $ExoU_{P.\ flu}$ and Gly-286 in $ExoU_{P.\ aer}$) are *highlighted*. *B,* charged surface and ribbon representations of the domain four portions of $ExoU_{P.\ flu}$ and $ExoU_{P.\ aer}$ and the corresponding portions of the PMT and *C. difficile* toxin B (*TcdB*). *Dashed yellow line* indicates a potential $PI(4,5)P_2$-binding/recognition site.

Although $PI(4,5)P_2$ binding domains are common among eukaryotic proteins, the ExoU MLD is only the second report of a bacterial $PI(4,5)P_2$ binding domain (72). Orth and co-workers (72) recently identified a bacterial phosphoinositide binding domain (BPD) in four effectors of the type III secretion systems of *Vibrio parahaemolyticus, Yersinia* spp., and *P. syringae*. The BPD localized these effectors to the plasma membrane of eukaryotic cells following injection. Unlike the MLD of ExoU, however, BPDs are at the N termini and overlap with the chaperone binding domains of these proteins. Structurally, BPDs have two β-strands and two α-helices instead of a four-helical bundle. These differences indicate that the ExoU MLD is quite distinct from the BPD and acts by a different mechanism. Perhaps this is because the PLA_2 activities of ExoU and other patatin-like proteins impose more stringent constraints, requiring that the MLDs not only localize to membranes but also provide access to phospholipid substrates in the membrane. In support of this, ExoU phospholipases appear to more closely mimic the strategy employed by some eukaryotic phospholipases, which use $PI(4,5)P_2$ to regulate not only their localization but also their activity. For instance, phospholipase D contains both a dedicated PH domain and an additional $PI(4,5)P_2$-binding site responsible for activation of its phospholipase activity (73). $cPLA_2$ is also localized to and activated by $PI(4,5)P_2$, further illustrating the important role of $PI(4,5)P_2$ in both intracellular targeting and activation of eukaryotic phospholipases (74). ExoU strongly binds to $PI(4,5)P_2$, with a K_d of just 110 nM, comparable with the PH domain of phospholipase C, a proto-

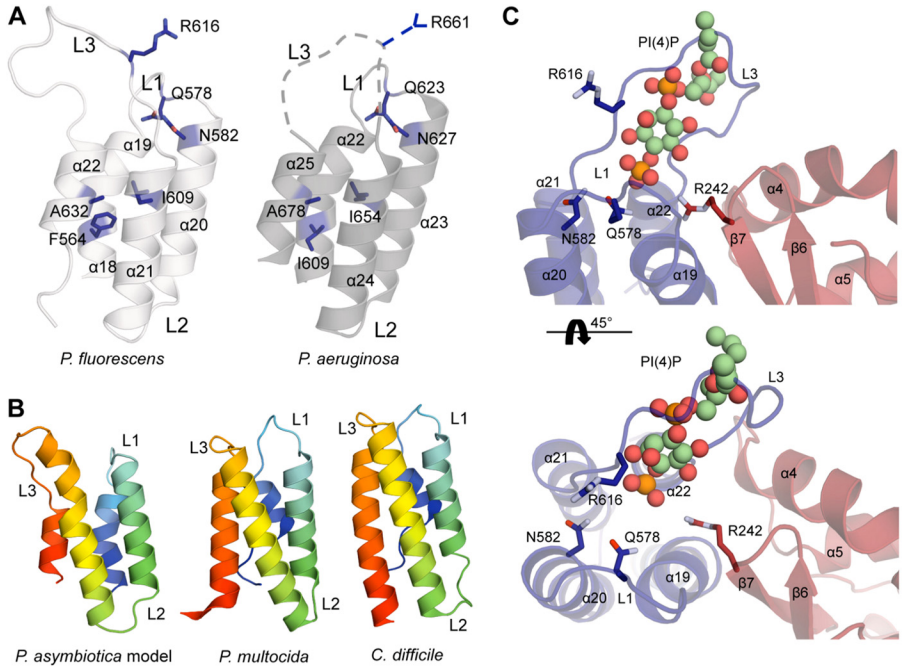

FIGURE 11. **Four-helical bundle structures of ExoU MLDs.** *A,* domain 4 structures of ExoU$_{P.\ flu}$ and ExoU$_{P.\ aer}$. Residues critical to PI(4,5)P_2 binding by ExoU$_{P.\ aer}$ (Fig. 1*B*) are indicated, as are the homologous residues present in ExoU$_{P.\ flu}$. The L3 of ExoU$_{P.\ aer}$, which contains Arg-661 (*blue dashed line*), was disordered, but the corresponding L3 of ExoU$_{P.\ flu}$ was ordered. *B,* depictions of the four-helical bundle structures of ExoU$_{P.\ asy}$, PMT, and *TcdB*. The ExoU$_{P.\ asy}$ structure is a model derived from the ExoU$_{P.\ aer}$ MLD (*rainbow colors*; *blue,* N terminus and *red,* C terminus). *C,* ExoU$_{P.\ flu}$ (colored as in Fig. 8*B*) with modeled PI(4)P molecule (*ball-and-stick model* with carbon atoms in *green*) based on the *L. pneumophila* effector DrrA/SidM structure (DrrA/SidM omitted for clarity; Protein Data Bank code 4MXP).

type mammalian PI(4,5)P_2 binding domain (75). It will be interesting to see whether eukaryotic PI(4,5)P_2 binding domains can substitute for the MLD of ExoU or whether the structural uniqueness of the MLD confers specific PI(4,5)P_2-binding properties that facilitate cell lysis by ExoU. In this regard, it should be noted that artificial targeting to eukaryotic membranes by farnesylation was insufficient to restore cell lysis to an ExoU variant with a disrupted MLD (30).

By obtaining the full-length crystal structure of a second ExoU patatin-like phospholipase, we were able to compare these two members of this protein family (28). In particular, the MLDs of ExoU$_{P.\ aer}$ and ExoU$_{P.\ flu}$ were quite similar, illustrating a conserved four-helical bundle fold that is important for PI(4,5)P_2 binding. PI(4,5)P_2 binding domains frequently contain positively charged residues that interact with the negatively charged phosphates of PI(4,5)P_2 (71). Our findings suggest that Arg-661 of ExoU$_{P.\ aer}$ is such a residue. In a previous examination of ExoU$_{P.\ aer}$ for important MLD residues, a substitution in Arg-661 significantly attenuated ExoU localization and cytotoxicity (30). In this study, the homologous Arg-616 residue of ExoU$_{P.\ flu}$ was also important for localization, and both residues were contained within the L3 loop of the four-helical bundle. Additionally, modeling of the ExoU$_{P.\ asy}$ MLD structure based on the previously characterized ExoU$_{P.\ aer}$ structure indicated that it too could form a four-helical bundle containing the conserved arginine in the L3 loop (Fig. 11*B*). This is consistent with its similar localization pattern, as well as the importance of its conserved arginine residue for localization. Interestingly, other unrelated bacterial toxins, such as *P. multocida* PMT and *C. difficile* TcdB, also contain four-helical bundles (Fig. 11*B*) (8, 76), but these proteins have different lipid-binding specificities. Unlike ExoU$_{P.aer}$ and ExoU$_{P.\ flu}$, PMT and TcdB bind with high affinity to a variety of negatively charged phospholipids such as phosphatidylserine and phosphatidylinositol (8, 38). Substitutions of positively charged amino acids in both the L1 and L3 loops of PMT and TcdB resulted in disruption of localization to membranes rich in these phospholipids (38). These other proteins also have conserved hydrophobic residues in the L3 loops that help establish membrane binding (38). ExoU does have hydrophobic residues in its L3 loop (residues 660–672), but they are not well conserved, suggesting they may not play a major role in localization (Fig. 3*A*).

The similarities between the four-helical bundles of the ExoU homologs and the other bacterial toxins suggest that four-helical bundles are a conserved structural platform for binding phospholipids in membranes but that alterations within these domains (and in particular in their L1 and L3 loops) "customize" their lipid-binding specificities. It will be interesting to see whether other four-helical bundle proteins are tailored to recognize phosphoinositides characteristic of other intracellular membrane compartments.

A more detailed mechanism of MLD binding will require a crystal structure of ExoU in complex with PI(4,5)P_2. Although such a structure is not yet available, the structure of the *Legionella pneumophila* toxin DrrA in complex with PI(4)P was recently solved (77). The membrane-binding portion of DrrA forms a three-helical bundle rather than a four-helical bundle, and the structure shows binding to PI(4)P rather than PI(4,5)P_2, but we reasoned that the comparison may nevertheless be informative. For this reason, we used this structure to model ExoU$_{P.\ flu}$ binding to PI(4)P. Superposition of the helical bundle domains positioned PI(4)P within the immediate vicinity of the

L3 loop with the conserved Arg-616 of $ExoU_{P.\ flu}$, as we had postulated (Fig. 11*C*). This supports the importance of the L3 loop and Arg-616 of $ExoU_{P.\ flu}$ in direct $PI(4,5)P_2$ binding and plasma membrane localization. Additional contacts outside the MLD may contribute to this binding, as Arg-242 (Arg-293 of $ExoU_{P.\ aer}$) is also well positioned to bind $PI(4,5)P_2$ (Fig. 10*B*). However, the MLD alone is sufficient for $PI(4,5)P_2$ binding (Fig. 1*A*) and for localization (Fig. 4). A more comprehensive screen is necessary to determine other residues in the L3 loop and the four-helical bundle of ExoU necessary for $PI(4,5)P_2$ binding and the potential contribution of residues within the MLD but outside the four-helical bundle or outside the MLD (27). These studies could help inform the differences in apparent affinity for $PI(4,5)P_2$ by the ExoU homologs, despite their maintaining a conserved mechanism (Fig. 2*D*). Of the several other residues already demonstrated to be important for $PI(4,5)P_2$ binding by ExoU (Fig. 1*B*), most were buried within the four-helical bundle and not located near the postulated membrane-binding interface (28). It is possible that Arg-661 (of $ExoU_{P.\ aer}$) makes initial contact with $PI(4,5)P_2$, causing a conformational change in the four-helical bundle, which allows these buried residues to contact the membrane. Alternatively, these other residues may play a structural role in helical packing and maintenance of the overall four-helical conformation, as has been postulated for critical residues in other four-helical bundle MLDs (29).

$ExoU_{P.\ aer}$ has been extensively investigated for its importance both clinically and in animal models of infection (23, 78). In contrast, the homologous ExoU proteins from the emerging human and insect pathogen *P. asymbiotica* and the plant commensal *P. fluorescens* have not been previously studied. Although these proteins need to be examined more thoroughly in the context of the bacteria that naturally produce them, several features suggest that they may be important for interaction with eukaryotic cells. First, they are postulated to be effector proteins of type III secretion systems, suggesting that they are injected into eukaryotic cells. Indeed, $ExoU_{P.\ asy}$ is the sole identified putative effector in the *P. asymbiotica* type III secretion system locus (59). Second, they localize by binding to $PI(4,5)P_2$, which is only found in eukaryotic cells. Third, they have PLA_2 activities that are modulated by eukaryotic factors, which, at least in the case of $ExoU_{P.\ aer}$, is used to subvert a broad spectrum of eukaryotic cells (79, 80). Interestingly, the enzymatic properties of these ExoU homologs differed substantially despite quite similar structures (Fig. 6). For example, compared with $ExoU_{P.\ aer}$, $ExoU_{P.\ flu}$ was active in the absence of co-activators and highly active in the presence of ubiquitin. A more detailed and expanded comparative structural analysis of similar MLD-containing patatin-like proteins may identify mechanistic explanations for the different enzymatic properties of this family of proteins.

In summary, we have characterized a $PI(4,5)P_2$ binding domain used by proteins from several different bacteria, including human and insect pathogens and a plant saprophyte. The four-helical bundle of the ExoU MLD binds $PI(4,5)P_2$ through a mechanism that requires a conserved arginine in an exposed loop. It will be interesting to determine whether proteins other than patatin-like phospholipases use similar MLD domains to bind $PI(4,5)P_2$.

Acknowledgments—We thank Peter Mayinger for the yeast strains, Kim Orth for the GFP-PH yeast expression construct, and Joyce Loper for the P. fluorescens strain. We thank members of the Hauser Laboratory for critical reading of the manuscript and the Northwestern University Cell Imaging Facility for assistance with microscopy. We thank the staff of the LS-CAT 21-ID-G station for help during x-ray data collection. Microscopy work utilized the Northwestern University Cell Imaging Facility, which is generously supported by National Institutes of Health Grant CCSG P30 CA060553 from NCI awarded to the Robert H. Lurie Comprehensive Cancer Center. The Center for Structural Genomics of Infectious Diseases project has been funded in whole or in part by National Institutes of Health through Contracts HHSN272200700058C and HHSN272201200026C from the NIAID and the Department of Health and Human Services (to W. F. A.).

Note Added in Proof—During the revision of this manuscript, Anderson *et al*. published an article (Anderson, D. M., Sato, H., Dirck, A. T., Feix, J. B., and Frank, D. W. (2014) *J. Bacteriol.* 10.1128/JB.02402-14) also demonstrating that some ExoU homologs bind $PI(4,5)P_2$ and are cytotoxic and that ubiquitin and $PI(4,5)P_2$ differentially activate these homologs.

REFERENCES

1. Tseng, T. T., Tyler, B. M., and Setubal, J. C. (2009) Protein secretion systems in bacterial-host associations, and their description in the Gene Ontology. *BMC Microbiol.* **9,** Suppl. 1, S2
2. Aktories, K. (2011) Bacterial protein toxins that modify host regulatory GTPases. *Nat. Rev. Microbiol.* **9,** 487–498
3. Satchell, K. J. (2009) Actin crosslinking toxins of Gram-negative bacteria. *Toxins* **1,** 123–133
4. Sitkiewicz, I., Stockbauer, K. E., and Musser, J. M. (2007) Secreted bacterial phospholipase A2 enzymes: better living through phospholipolysis. *Trends Microbiol.* **15,** 63–69
5. Geissler, B. (2012) Bacterial toxin effector-membrane targeting: outside in, then back again. *Front. Cell. Infect. Microbiol.* **2,** 75
6. Chen, S., and Barbieri, J. T. (2011) Association of botulinum neurotoxin serotype A light chain with plasma membrane-bound SNAP-25. *J. Biol. Chem.* **286,** 15067–15072
7. Boucrot, E., Beuzón, C. R., Holden, D. W., Gorvel, J. P., and Méresse, S. (2003) *Salmonella typhimurium* SifA effector protein requires its membrane-anchoring C-terminal hexapeptide for its biological function. *J. Biol. Chem.* **278,** 14196–14202
8. Kamitani, S., Kitadokoro, K., Miyazawa, M., Toshima, H., Fukui, A., Abe, H., Miyake, M., and Horiguchi, Y. (2010) Characterization of the membrane-targeting C1 domain in *Pasteurella multocida* toxin. *J. Biol. Chem.* **285,** 25467–25475
9. Zhang, Y., Deng, Q., Porath, J. A., Williams, C. L., Pederson-Gulrud, K. J., and Barbieri, J. T. (2007) Plasma membrane localization affects the RhoGAP specificity of *Pseudomonas* ExoS. *Cell. Microbiol.* **9,** 2192–2201
10. Hirschberg, H. J., Simons, J. W., Dekker, N., and Egmond, M. R. (2001) Cloning, expression, purification and characterization of patatin, a novel phospholipase A. *Eur. J. Biochem.* **268,** 5037–5044
11. Sato, H., Frank, D. W., Hillard, C. J., Feix, J. B., Pankhaniya, R. R., Moriyama, K., Finck-Barbançon, V., Buchaklian, A., Lei, M., Long, R. M., Wiener-Kronish, J., and Sawa, T. (2003) The mechanism of action of the *Pseudomonas aeruginosa*-encoded type III cytotoxin, ExoU. *EMBO J.* **22,** 2959–2969
12. Lang, C., and Flieger, A. (2011) Characterisation of *Legionella pneumophila* phospholipases and their impact on host cells. *Eur. J. Cell Biol.* **90,** 903–912
13. Banerji, S., and Flieger, A. (2004) Patatin-like proteins: a new family of lipolytic enzymes present in bacteria? *Microbiology* **150,** 522–525
14. Salacha, R., Kovacipć, F., Brochier-Armanet, C., Wilhelm, S., Tommassen,

J., Filloux, A., Voulhoux, R., and Bleves, S. (2010) The *Pseudomonas aeruginosa* patatin-like protein PlpD is the archetype of a novel type V secretion system. *Environ. Microbiol.* **12,** 1498–1512
15. VanRheenen, S. M., Luo, Z. Q., O'Connor, T., and Isberg, R. R. (2006) Members of a *Legionella pneumophila* family of proteins with ExoU (phospholipase A) active sites are translocated to target cells. *Infect. Immun.* **74,** 3597–3606
16. Aurass, P., Pless, B., Rydzewski, K., Holland, G., Bannert, N., and Flieger, A. (2009) bdhA-patD operon as a virulence determinant, revealed by a novel large-scale approach for identification of *Legionella pneumophila* mutants defective for amoeba infection. *Appl. Environ. Microbiol.* **75,** 4506–4515
17. Laskowski, R. A., MacArthur, M. W., Moss, D. S., and Thornton, J. M. (1993) PROCHECK: a program to check the stereochemical quality of protein structures. *J. Appl. Crystallogr.* **26,** 283–291
18. Zhu, W., Hammad, L. A., Hsu, F., Mao, Y., and Luo, Z. Q. (2013) Induction of caspase 3 activation by multiple *Legionella pneumophila* Dot/Icm substrates. *Cell. Microbiol.* **15,** 1783–1795
19. Kang, P. J., Hauser, A. R., Apodaca, G., Fleiszig, S. M., Wiener-Kronish, J., Mostov, K., and Engel, J. N. (1997) Identification of *Pseudomonas aeruginosa* genes required for epithelial cell injury. *Mol. Microbiol.* **24,** 1249–1262
20. Hauser, A. R., Kang, P. J., and Engel, J. (1998) PepA, a novel secreted protein of *Pseudomonas aeruginosa,* is necessary for cytotoxicity and virulence. *Mol. Microbiol.* **27,** 807–818
21. Finck-Barbançon, V., Goranson, J., Zhu, L., Sawa, T., Wiener-Kronish, J. P., Fleiszig, S. M., Wu, C., Mende-Mueller, L., and Frank, D. W. (1997) ExoU expression by *Pseudomonas aeruginosa* correlates with acute cytotoxicity and epithelial injury. *Mol. Microbiol.* **25,** 547–557
22. Hauser, A. R., Cobb, E., Bodi, M., Mariscal, D., Vallés, J., Engel, J. N., and Rello, J. (2002) Type III protein secretion is associated with poor clinical outcomes in patients with ventilator-associated pneumonia caused by *Pseudomonas aeruginosa*. *Crit. Care Med.* **30,** 521–528
23. Schulert, G. S., Feltman, H., Rabin, S. D., Martin, C. G., Battle, S. E., Rello, J., and Hauser, A. R. (2003) Secretion of the toxin ExoU is a marker for highly virulent *Pseudomonas aeruginosa* isolates obtained from patients with hospital-acquired pneumonia. *J. Infect. Dis.* **188,** 1695–1706
24. Sato, H., Feix, J. B., Hillard, C. J., and Frank, D. W. (2005) Characterization of phospholipase activity of the *Pseudomonas aeruginosa* type III cytotoxin, ExoU. *J. Bacteriol.* **187,** 1192–1195
25. Anderson, D. M., Schmalzer, K. M., Sato, H., Casey, M., Terhune, S. S., Haas, A. L., Feix, J. B., and Frank, D. W. (2011) Ubiquitin and ubiquitin-modified proteins activate the *Pseudomonas aeruginosa* T3SS cytotoxin, ExoU. *Mol. Microbiol.* **82,** 1454–1467
26. Tyson, G. H., and Hauser, A. R. (2013) Phosphatidylinositol 4,5-bisphosphate is a novel co-activator of the *Pseudomonas aeruginosa* cytotoxin ExoU. *Infect. Immun.* **81,** 2873–2881
27. Rabin, S. D., Veesenmeyer, J. L., Bieging, K. T., and Hauser, A. R. (2006) A C-terminal domain targets the *Pseudomonas aeruginosa* cytotoxin ExoU to the plasma membrane of host cells. *Infect. Immun.* **74,** 2552–2561
28. Halavaty, A. S., Borek, D., Tyson, G. H., Veesenmeyer, J. L., Shuvalova, L., Minasov, G., Otwinowski, Z., Hauser, A. R., and Anderson, W. F. (2012) Structure of the type III secretion effector protein ExoU in complex with its chaperone SpcU. *PLoS One* **7,** e49388
29. Geissler, B., Tungekar, R., and Satchell, K. J. (2010) Identification of a conserved membrane localization domain within numerous large bacterial protein toxins. *Proc. Natl. Acad. Sci. U.S.A.* **107,** 5581–5586
30. Veesenmeyer, J. L., Howell, H., Halavaty, A. S., Ahrens, S., Anderson, W. F., and Hauser, A. R. (2010) Role of the membrane localization domain of the *Pseudomonas aeruginosa* effector protein ExoU in cytotoxicity. *Infect. Immun.* **78,** 3346–3357
31. Gendrin, C., Contreras-Martel, C., Bouillot, S., Elsen, S., Lemaire, D., Skoufias, D. A., Huber, P., Attree, I., and Dessen, A. (2012) Structural basis of cytotoxicity mediated by the type III secretion toxin ExoU from *Pseudomonas aeruginosa*. *PLoS Pathog.* **8,** e1002637
32. Sato, H., and Frank, D. W. (2014) Intoxication of host cells by the T3SS phospholipase ExoU: PI(4,5)P2-associated, cytoskeletal collapse and late phase membrane blebbing. *PLoS One* **9,** e103127
33. McLaughlin, S., Wang, J., Gambhir, A., and Murray, D. (2002) PIP(2) and proteins: interactions, organization, and information flow. *Annu. Rev. Biophys. Biomol. Struct.* **31,** 151–175
34. Behnia, R., and Munro, S. (2005) Organelle identity and the signposts for membrane traffic. *Nature* **438,** 597–604
35. Hamada, K., Shimizu, T., Matsui, T., Tsukita, S., and Hakoshima, T. (2000) Structural basis of the membrane-targeting and unmasking mechanisms of the radixin FERM domain. *EMBO J.* **19,** 4449–4462
36. Lemmon, M. A., and Ferguson, K. M. (2000) Signal-dependent membrane targeting by pleckstrin homology (PH) domains. *Biochem. J.* **350,** 1–18
37. Rabin, S. D., and Hauser, A. R. (2003) Pseudomonas aeruginosa ExoU, a toxin transported by the type III secretion system, kills *Saccharomyces cerevisiae*. *Infect. Immun.* **71,** 4144–4150
38. Geissler, B., Ahrens, S., and Satchell, K. J. (2012) Plasma membrane association of three classes of bacterial toxins is mediated by a basic-hydrophobic motif. *Cell. Microbiol.* **14,** 286–298
39. Altschul, S. F., Gish, W., Miller, W., Myers, E. W., and Lipman, D. J. (1990) Basic local alignment search tool. *J. Mol. Biol.* **215,** 403–410
40. Kim, H., Afsari, H. S., and Cho, W. (2013) High-throughput fluorescence assay for membrane-protein interaction. *J. Lipid Res.* **54,** 3531–3538
41. Otwinowski, Z., and Minor, W. (1997) Processing of X-ray diffraction data collected in oscillation mode. *Methods Enzymol.* **276,** 307–326
42. McCoy, A. J., Grosse-Kunstleve, R. W., Adams, P. D., Winn, M. D., Storoni, L. C., and Read, R. J. (2007) Phaser crystallographic software. *J. Appl. Crystallogr.* **40,** 658–674
43. Winn, M. D., Ballard, C. C., Cowtan, K. D., Dodson, E. J., Emsley, P., Evans, P. R., Keegan, R. M., Krissenel, E. B., Leslie, A. G., McCoy, A., McNicholas, S. J., Murshudov, G. N., Pannu, N. S., Potterton, E. A., Powell, H. R., Read, R. J., Vagin, A., and Wilson, K. S. (2011) Overview of the CCP4 suite and current developments. *Acta Crystallogr. D Biol. Crystallogr.* **67,** 235–242
44. Morris, R. J., Perrakis, A., and Lamzin, V. S. (2003) ARP/warp and automatic interpretation of protein electron density maps. *Methods Enzymol.* **374,** 229–244
45. Murshudov, G. N., Skubák, P., Lebedev, A. A., Pannu, N. S., Steiner, R. A., Nicholls, R. A., Winn, M. D., Long, F., and Vagin, A. A. (2011) REFMAC5 for the refinement of macromolecular crystal structures. *Acta Crystallogr. D Biol. Crystallogr.* **67,** 355–367
46. Emsley, P., and Cowtan, K. (2004) Coot: model-building tools for molecular graphics. *Acta Crystallogr. D Biol. Crystallogr.* **60,** 2126–2132
47. Emsley, P., Lohkamp, B., Scott, W. G., and Cowtan, K. (2010) Features and development of Coot. *Acta Crystallogr. D Biol. Crystallogr.* **66,** 486–501
48. Chen, V. B., Arendall, W. B., 3rd, Headd, J. J., Keedy, D. A., Immormino, R. M., Kapral, G. J., Murray, L. W., Richardson, J. S., and Richardson, D. C. (2010) MolProbity: all-atom structure validation for macromolecular crystallography. *Acta Crystallogr. D Biol. Crystallogr.* **66,** 12–21
49. Davis, I. W., Leaver-Fay, A., Chen, V. B., Block, J. N., Kapral, G. J., Wang, X., Murray, L. W., Arendall, W. B., 3rd, Snoeyink, J., Richardson, J. S., and Richardson, D. C. (2007) MolProbity: all-atom contacts and structure validation for proteins and nucleic acids. *Nucleic Acids Res.* **35,** W375–W383
50. Krissinel, E., and Henrick, K. (2007) Inference of macromolecular assemblies from crystalline state. *J. Mol. Biol.* **372,** 774–797
51. DeLano, W. L. (2012) *The PyMOL Molecular Graphics System,* Version 1.5.0.4, Schrödinger, LLC, New York
52. Mesmin, B., Robbe, K., Geny, B., Luton, F., Brandolin, G., Popoff, M. R., and Antonny, B. (2004) A phosphatidylserine-binding site in the cytosolic fragment of *Clostridium sordellii* lethal toxin facilitates glucosylation of membrane-bound Rac and is required for cytotoxicity. *J. Biol. Chem.* **279,** 49876–49882
53. Szentpetery, Z., Balla, A., Kim, Y. J., Lemmon, M. A., and Balla, T. (2009) Live cell imaging with protein domains capable of recognizing phosphatidylinositol 4,5-bisphosphate; a comparative study. *BMC Cell Biol.* **10,** 67
54. Hammond, G. R., Fischer, M. J., Anderson, K. E., Holdich, J., Koteci, A., Balla, T., and Irvine, R. F. (2012) PI4P and PI(4,5)P2 are essential but independent lipid determinants of membrane identity. *Science* **337,** 727–730
55. Chen, Y., Sheng, R., Källberg, M., Silkov, A., Tun, M. P., Bhardwaj, N., Kurilova, S., Hall, R. A., Honig, B., Lu, H., and Cho, W. (2012) Genome-wide functional annotation of dual-specificity protein- and lipid-binding modules that regulate protein interactions. *Mol. Cell* **46,** 226–237

56. Várnai, P., and Balla, T. (2008) Live cell imaging of phosphoinositides with expressed inositide binding protein domains. *Methods* **46,** 167–176
57. Manna, D., Bhardwaj, N., Vora, M. S., Stahelin, R. V., Lu, H., and Cho, W. (2008) Differential roles of phosphatidylserine, PtdIns(4,5)P2, and PtdIns(3,4,5)P3 in plasma membrane targeting of C2 domains. Molecular dynamics simulation, membrane binding, and cell translocation studies of the PKCα C2 domain. *J. Biol. Chem.* **283,** 26047–26058
58. Varivarn, K., Champa, L. A., Silby, M. W., and Robleto, E. A. (2013) Colonization strategies of *Pseudomonas fluorescens* Pf0–1: activation of soil-specific genes important for diverse and specific environments. *BMC Microbiol.* **13,** 92
59. Costa, S. C., Girard, P. A., Brehélin, M., and Zumbihl, R. (2009) The emerging human pathogen *Photorhabdus asymbiotica* is a facultative intracellular bacterium and induces apoptosis of macrophage-like cells. *Infect. Immun.* **77,** 1022–1030
60. Loper, J. E., Hassan, K. A., Mavrodi, D. V., Davis, E. W., 2nd, Lim, C. K., Shaffer, B. T., Elbourne, L. D., Stockwell, V. O., Hartney, S. L., Breakwell, K., Henkels, M. D., Tetu, S. G., Rangel, L. I., Kidarsa, T. A., Wilson, N. L., van de Mortel, J. E., Song, C., Blumhagen, R., Radune, D., Hostetler, J. B., Brinkac, L. M., Durkin, A. S., Kluepfel, D. A., Wechter, W. P., Anderson, A. J., Kim, Y. C., Pierson, L. S., 3rd, Pierson, E. A., Lindow, S. E., Kobayashi, D. Y., Raaijmakers, J. M., Weller, D. M., Thomashow, L. S., Allen, A. E., and Paulsen, I. T. (2012) Comparative genomics of plant-associated *Pseudomonas* spp.: insights into diversity and inheritance of traits involved in multitrophic interactions. *PLoS Genet.* **8,** e1002784
61. Wiradjaja, F., Ooms, L. M., Tahirovic, S., Kuhne, E., Devenish, R. J., Munn, A. L., Piper, R. C., Mayinger, P., and Mitchell, C. A. (2007) Inactivation of the phosphoinositide phosphatases Sac1p and Inp54p leads to accumulation of phosphatidylinositol 4,5-bisphosphate on vacuole membranes and vacuolar fusion defects. *J. Biol. Chem.* **282,** 16295–16307
62. Goujon, M., McWilliam, H., Li, W., Valentin, F., Squizzato, S., Paern, J., and Lopez, R. (2010) A new bioinformatics analysis tools framework at EMBL-EBI. *Nucleic Acids Res.* **38,** W695–W699
63. Holm, L., and Park, J. (2000) DaliLite workbench for protein structure comparison. *Bioinformatics* **16,** 566–567
64. McWilliam, H., Li, W., Uludag, M., Squizzato, S., Park, Y. M., Buso, N., Cowley, A. P., and Lopez, R. (2013) Analysis tool web services from the EMBL-EBI. *Nucleic Acids Res.* **41,** W597–W600
65. Rabin, S. D., and Hauser, A. R. (2005) Functional regions of the *Pseudomonas aeruginosa* cytotoxin ExoU. *Infect Immun.* **73,** 573–582
66. Bishé, B., Syed, G. H., Field, S. J., and Siddiqui, A. (2012) Role of phosphatidylinositol 4-phosphate (PI4P) and its binding protein GOLPH3 in hepatitis C virus secretion. *J. Biol. Chem.* **287,** 27637–27647
67. Gillooly, D. J., Morrow, I. C., Lindsay, M., Gould, R., Bryant, N. J., Gaullier, J. M., Parton, R. G., and Stenmark, H. (2000) Localization of phosphatidylinositol 3-phosphate in yeast and mammalian cells. *EMBO J.* **19,** 4577–4588
68. Itoh, T., Koshiba, S., Kigawa, T., Kikuchi, A., Yokoyama, S., and Takenawa, T. (2001) Role of the ENTH domain in phosphatidylinositol-4,5-bisphosphate binding and endocytosis. *Science* **291,** 1047–1051
69. Chen, X., and Rotenberg, S. A. (2010) PhosphoMARCKS drives motility of mouse melanoma cells. *Cell. Signal.* **22,** 1097–1103
70. Martin, T. F. (2001) PI(4,5)P(2) regulation of surface membrane traffic. *Curr. Opin. Cell Biol.* **13,** 493–499
71. Li, L., Shi, X., Guo, X., Li, H., and Xu, C. (2014) Ionic protein-lipid interaction at the plasma membrane: what can the charge do? *Trends Biochem. Sci.* **39,** 130–140
72. Salomon, D., Guo, Y., Kinch, L. N., Grishin, N. V., Gardner, K. H., and Orth, K. (2013) Effectors of animal and plant pathogens use a common domain to bind host phosphoinositides. *Nat. Commun.* **4,** 2973
73. Sciorra, V. A., Rudge, S. A., Prestwich, G. D., Frohman, M. A., Engebrecht, J., and Morris, A. J. (1999) Identification of a phosphoinositide binding motif that mediates activation of mammalian and yeast phospholipase D isoenzymes. *EMBO J.* **18,** 5911–5921
74. Le Berre, L., Takano, T., Papillon, J., Lemay, S., and Cybulsky, A. V. (2006) Role of phosphatidylinositol 4,5-bisphosphate in the activation of cytosolic phospholipase A2-α. *Prostaglandins Other Lipid Mediat.* **81,** 113–125
75. Yoon, Y., Lee, P. J., Kurilova, S., and Cho, W. (2011) *In situ* quantitative imaging of cellular lipids using molecular sensors. *Nat. Chem.* **3,** 868–874
76. Reinert, D. J., Jank, T., Aktories, K., and Schulz, G. E. (2005) Structural basis for the function of *Clostridium difficile* toxin B. *J. Mol. Biol.* **351,** 973–981
77. Del Campo, C. M., Mishra, A. K., Wang, Y. H., Roy, C. R., Janmey, P. A., and Lambright, D. G. (2014) Structural basis for PI(4)P-specific membrane recruitment of the legionella pneumophila effector DrrA/SidM. *Structure* **22,** 397–408
78. Shaver, C. M., and Hauser, A. R. (2004) Relative contributions of *Pseudomonas aeruginosa* ExoU, ExoS, and ExoT to virulence in the lung. *Infect Immun.* **72,** 6969–6977
79. Matz, C., Moreno, A. M., Alhede, M., Manefield, M., Hauser, A. R., Givskov, M., and Kjelleberg, S. (2008) *Pseudomonas aeruginosa* uses type III secretion system to kill biofilm-associated amoebae. *ISME J.* **2,** 843–852
80. Miyata, S., Casey, M., Frank, D. W., Ausubel, F. M., and Drenkard, E. (2003) Use of the *Galleria mellonella* caterpillar as a model host to study the role of the type III secretion system in *Pseudomonas aeruginosa* pathogenesis. *Infect. Immun.* **71,** 2404–2413
81. Schorr, M., Then, A., Tahirovic, S., Hug, N., and Mayinger, P. (2001) The phosphoinositide phosphatase Sac1p controls trafficking of the yeast Chs3p chitin synthase. *Curr. Biol.* **11,** 1421–1426